This is a post-print (revised author version) of the article

Graf A et al. 2020 Altered energy partitioning across terrestrial ecosystems in the European drought year 2018. Phil. Trans. R. Soc. B 375: 20190524. http://dx.doi.org/10.1098/rstb.2019.0524

published in Philosophical Transactions of the Royal Society B, theme issue 'Impacts of the 2018 severe drought and heatwave in Europe: from site to continental scale', 2020, DOI https://doi.org/10.1098/rstb.2019.0524. Please be aware that few details generally not affecting the scientific content may differ towards the fully proof-edited, official journal version; in particular page numbers are not convertible.

# Altered energy partitioning across terrestrial ecosystems in the European drought year 2018

Alexander Graf[1,*], Anne Klosterhalfen[2,1], Nicola Arriga[3], Christian Bernhofer[4], Heye Bogena[1], Frédéric Bornet[5], Nicolas Brüggemann[1], Christian Brümmer[6], Nina Buchmann[7], Jinshu Chi[2], Christophe Chipeaux[8], Edoardo Cremonese[9], Matthias Cuntz[10], Jiří Dušek[11], Tarek S. El-Madany[12], Silvano Fares[13], Milan Fischer[11], Lenka Foltýnová[11], Mana Gharun[7], Shiva Ghiasi[7], Bert Gielen[14], Pia Gottschalk[15], Thomas Grünwald[4], Günther Heinemann[16], Bernard Heinesch[17], Michal Heliasz[18], Jutta Holst[18], Lukas Hörtnagl[7], Andreas Ibrom[19], Joachim Ingwersen[20], Gerald Jurasinski[21], Janina Klatt[22], Alexander Knohl[23], Franziska Koebsch[21], Jan Konopka[24], Mika Korkiakoski[25], Natalia Kowalska[11], Pascal Kremer[20], Bart Kruijt[26], Sebastien Lafont[8], Joël Léonard[5], Anne De Ligne[17], Bernard Longdoz[17], Denis Loustau[8], Vincenzo Magliulo[27], Ivan Mammarella[28], Giovanni Manca[3], Matthias Mauder[22], Mirco Migliavacca[12], Meelis Mölder[18], Johan Neirynck[29], Patrizia Ney[1], Mats Nilsson[2], Eugénie Paul-Limoges[30], Matthias Peichl[2], Andrea Pitacco[31], Arne Poyda[20,32], Corinna Rebmann[33], Marilyn Roland[14], Torsten Sachs[15], Marius Schmidt[1], Frederik Schrader[6], Lukas Siebicke[23], Ladislav Šigut[11], Eeva-Stiina Tuittila[34], Andrej Varlagin[35], Nadia Vendrame[31], Caroline Vincke[36], Ingo Völksch[22], Stephan Weber[24], Christian Wille[15], Hans-Dieter Wizemann[37], Matthias Zeeman[22], Harry Vereecken[1]

*[1]Institute of Bio- and Geosciences: Agrosphere (IBG-3), Forschungszentrum Jülich, Wilhelm-Johnen-Straße, 52428 Jülich, Germany, correspondence: a.graf@fz-juelich.de; [2]Department of Forest Ecology and Management, Swedish University of Agricultural Sciences, Skogsmarksgränd 17, 901 83 Umeå, Sweden; [3]European Commission, Joint Research Centre (JRC), Ispra, Italy; [4]Chair of Meteorology, Technische Universität Dresden, Pienner Str. 23, 01737 Tharandt, Germany; [5]BioEcoAgro Joint Research Unit, INRAE, Université de Liège, Université de Lille, Université de Picardie Jules Verne, 02000, Barenton-Bugny, France; [6]Thünen Institute of Climate-Smart Agriculture, Bundesallee 65, 38116 Braunschweig, Germany; [7]Department of Environmental Systems Science, ETH Zurich, Universitaetstrasse 2, 8092 Zurich, Switzerland; [8]ISPA, Bordeaux Sciences Agro, INRAE, F-33140, Villenave d'Ornon, France; [9]Climate Change Unit, Environmental Protection Agency of Aosta Valley, Italy; [10]Unité mixte de Recherche Silva, Université de Lorraine, AgroParisTech, INRA, UMR Silva, 54000 Nancy, France; [11]Department of Matter and Energy Fluxes, Global Change Research Institute of the Czech Academy of Sciences, Bělidla 986/4a, 60300 Brno, Czech Republic; [12]Max Planck Institute for Biogeochemistry Department Biogeochemical Integration Hans-Knöll-Str. 10 07745 Jena Germany; [13]National Research Council (CNR), Institute of Bioeconomy, Via dei Taurini 19, 00100 Rome, Italy; [14]University of Antwerp, Plants and Ecosystems, Universiteitsplein 1, 2610 Wilrijk, Belgium; [15]Remote Sensing and Geoinformatics, German Research Centre for Geosciences (GFZ), Telegrafenberg, 14473 Potsdam, Germany; [16]Environmental Meteorology, University of Trier, Behringstr. 21, 54296 Trier, Germany; [17]Terra Teaching and Research Centre , University of Liege – Gembloux Agro-Bio Tech, Avenue de la Faculté, 8, B-5030 Gembloux, Belgium; [18]Lund University, Department of Physical Geography and Ecosystem Science, Sölvegatan 12, 22362 Lund, Sweden; [19]Technical University of Denmark (DTU), Department of Environmental Engineering, Bygningstorvet 115, 2800 Lyngby, Denmark; [20]Institute of Soil Science and Land Evaluation, University of Hohenheim, Emil-Wolff-Str. 27, 70599 Stuttgart, Germany; [21]Department for Landscape Ecology and Site Evaluation, University of Rostock, Justus von Liebig Weg 6, 18059 Rostock, Germany; [22]Institute of Meteorology and Climate Research - Atmospheric Environmental Research, Karlsruhe Institute of Technology, Campus Alpin, Kreuzeckbahnstr. 19, 82467 Garmisch-Partenkirchen; [23]Bioclimatology, University of Goettingen, Büsgenweg 2, 37077 Goettingen, Germany;*

*[24]Climatology and Environmental Meteorology, Institute of Geoecology, Technische Universität Braunschweig, Langer Kamp 19c, 38106 Braunschweig; [25]Climate System Research Unit, Finnish Meteorological Institute, PO Box 503, 00101 Helsinki, Finland; [26]Department of Environmental Sciences, Wageningen University and Research, PO Box 47, 6700 AA Wageningen, The Netherlands; [27]CNR - Institute for Agricultural and Forest Systems, Via Patacca, 85, 80040, Ercolano (Napoli) Italy; [28]Institute for Atmospheric and Earth System Research/Physics, Faculty of Science, University of Helsinki, Gustaf Hällströmin katu 2B, FI-00014 Helsinki, Finland; [29]Department of Geography, University of Zurich, Winterthurerstrasse 190, 8057 Zurich, Switzerland; [29]Research Institute for Nature and Forest, INBO, Havenlaan 88 Box 73, 1000 Brussels, Belgium; [31]Department of Agronomy, Food, Natural resources, Animals and Environment, University of Padova, Viale dell'Università 16, 35020 Legnaro, Italy; [32]Institute of Crop Science and Plant Breeding, Grass and Forage Science/Organic Agriculture, Christian-Albrechts-University Kiel, Hermann-Rodewald-Str. 9, 24118 Kiel, Germany; [33]Helmholtz Centre for Environmental Research GmbH - UFZ, Department Computational Hydrosystems, Permoserstraße 15, 04318 Leipzig, Germany; [34]University of Eastern Finland, School of Forest Sciences, Yliopistokatu 7, FI-80101 Joensuu, Finland; [35]Laboratory of Biocenology, A.N. Severtsov Institute of Ecology and Evolution, Russian Academy of Sciences, Leninsky pr.33, Moscow 119071, Russia [36]Earth and Life Institute, Université catholique de Louvain, Environmental Sciences, 1348 Louvain-la-Neuve, Belgium; [37]Institute of Physics and Meteorology, University of Hohenheim, 70593 Stuttgart, Germany*

ORCIDs: AG, 0000-0003-4870-7622; AKl, 0000-0001-7999-8966; NBr, 0000-0003-3851-2418; CBr, 0000-0001-6621-5010; NBu, 0000-0003-0826-2980; JC, 0000-0001-5688-8895; CC, 0000-0003-0338-8517; EC, 0000-0002-6708-8532; MC, 0000-0002-5966-1829; TSE-M, 0000-0002-0726-7141; LF, 0000-0001-8202-955X; MG, 0000-0003-0337-7367; TG, 0000-0003-2263-0073; GH, 0000-0002-4831-9016; BH, 0000-0001-7594-6341; JH, 0000-0001-8719-1927; LH, 0000-0002-5569-0761; AI, 0000-0002-1341-921X; GJ, 0000-0002-6248-9388; AKn, 0000-0002-7615-8870; FK, 0000-0003-1045-7680; MK, 0000-0001-6875-9978; NK, 0000-0002-7366-7231; SL, 0000-0002-9605-8092; JL, 0000-0002-9907-9104; DL, 0000-0003-3990-400X; VM, 0000-0001-5505-6552; IM, 0000-0002-8516-3356; MMa, 0000-0002-8789-163X; MMi, 0000-0003-3546-8407; PN, 0000-0001-6821-8661; MP, 0000-0002-9940-5846; APi, 0000-0002-7260-6242; CR, 0000-0002-8665-0375; MR, 0000-0002-5770-3896; TS, 0000-0002-9959-4771; MS, 0000-0001-5292-7092; FS, 0000-0002-5668-3467; LŠ, 0000-0003-1951-4100; AV, 0000-0002-2549-5236; NV, 0000-0002-2772-6755; IV, 0000-0001-9700-2771; SW, 0000-0003-0335-4691; MZ, 0000-0001-9186-2519; HV, 0000-0002-8051-8517

**Keywords:** eddy-covariance, energy balance, evapotranspiration, heat flux, net carbon uptake, water-use efficiency

## Summary

Drought and heat events, such as the 2018 European drought, interact with the exchange of energy between the land surface and the atmosphere, potentially affecting albedo, sensible and latent heat fluxes, as well as $CO_2$ exchange. Each of these quantities may aggravate or mitigate the drought, heat, their side effects on productivity, water scarcity, and global warming. We utilized measurements of 56 eddy covariance sites across Europe to examine the response of fluxes to extreme drought prevailing most of the year 2018 and how the response differed across various ecosystem types (forests, grasslands, croplands and peatlands). Each component of the surface radiation and energy balance observed in 2018 was compared to available data per site during a reference period 2004-2017. Based on anomalies in precipitation and reference evapotranspiration, we classified 46 sites as drought-affected. These received on average 9% more solar radiation and released 32% more sensible heat to the atmosphere compared to the mean of the reference period. In general, drought decreased net $CO_2$ uptake by 17.8%, but did not significantly change net evapotranspiration. The response of these fluxes differed characteristically between ecosystems; in particular the general increase in evaporative index was strongest in peatlands and weakest in croplands.

# Introduction

Exceptionally dry and warm periods can serve as a testbed for the future response of the land surface to climate change, as they represent air temperature, net radiation ($R_n$), and regionally also precipitation ($P$) and incident solar radiation ($R_{si}$) levels that may occur more frequently in the future. Depending on their severity and duration, heat wave and soil water shortage episodes have been observed to dramatically reduce plant productivity, ecosystems' carbon balance and food, fiber and wood production in Europe, with an increasing frequency during the three last decades [1-3]. In contrast to distinct summer heat waves, in 2018 unusually warm conditions throughout most of Europe and dry conditions in its northern half started in spring and persisted throughout the remainder of the year [4], representing the largest annual soil moisture anomaly in the period 1979-2019 [5].

Higher $R_n$ enforces an increase in the sum of the turbulent sensible heat flux ($H$), latent heat flux ($\lambda ET$), heat stored in the ground, vegetation and water bodies ($S_l$) and energy converted chemically ($E_c$), particularly into biomass by photosynthetic $CO_2$ uptake or vice versa by respiration:

$$H + \lambda ET + S_l + E_c = R_n = (1 - \alpha)R_{si} - R_{lo} + R_{li} \quad (1.1)$$

Land surface albedo ($\alpha$), outgoing longwave radiation from the land surface ($R_{lo}$) and incoming longwave radiation from the atmosphere ($R_{li}$) co-determine the relation between $R_{si}$ and $R_n$.

A small increment in $R_n$ can increase any, and likely all, terms on the left-hand side of Equation 1. If sunny and dry conditions prevail, however, changes will be more diverse. The increase in $E_c$ may diminish as photosynthesis becomes limited by stomatal closure or biochemical limitations [6]. The same may happen to evapotranspiration ($ET$) as near-surface water for evaporation becomes depleted or stomatal closure limits transpiration. As stomatal closure or soil water shortage continue, plants may develop less green leaf area than usual or initiate senescence, eventually leading to a decrease in transpiration and $E_c$, as well as to a change in $\alpha$ and thus $R_n$. At the same time, soil water shortage can reduce soil respiration in spite of higher temperature, moderating the decrease in $E_c$, as shown for the 2003 drought and heat wave [1, 2]. If a warm anomaly is characterized by advection rather than by local production of atmospheric heat, $H$ might decrease according to the temperature difference between land surface and atmosphere. Hence, responses on the left-hand side of Equation 1 might differ in magnitude and sign between fluxes.

The objective of this study was to analyse the response of land surface-atmosphere energy fluxes to the exceptionally dry and warm conditions during the year 2018 at ecosystem monitoring sites across Europe. Based on the response mechanisms described above, we hypothesize that $S_l$ and $H$ are likely to consistently increase across different ecosystems. $ET$ and $E_c$, in contrast, may increase in response to increasing $R_n$ and $R_{si}$, respectively, or decrease in response to soil water depletion. $ET$ and $E_c$ are linked to each other by the drought response of the vegetation, but can partly decouple due to the role of soil respiration and evaporation. Each flux has a different effect on the atmosphere, e.g. direct heating through $H$, local cooling and nonlocal heating through $ET$, and long-term global cooling through the greenhouse effect of $E_c$ on $R_{li}$. Examining the ecosystem-dependent variability of $ET$ and $E_c$ responses, and their side effect on $H$, may help to understand how land use modulates local and global heating in response to droughts and heat waves [7]. In this study, we compared fluxes from equation (1.1) directly measured at 56 eddy-covariance [8] stations across Europe in 2018 to those in a reference period 2004-2017, discriminating between the ecosystem types forest, grassland, cropland and peatland.

# Methods

Meteorological data and fluxes [9] were originally provided as half-hourly averages, mostly in the framework of the ICOS (www.icos-ri.eu) and TERENO (www.tereno.net) networks [10, 11]. A site was selected for this study when sufficient data of the turbulent fluxes of sensible heat, water vapour, and $CO_2$ were available for 2018 and at least for one year from the reference period 2004 to 2017. All 14 reference years were available at seven sites, and only one reference year at four sites. The majority of sites were forest sites, ten were crop sites, nine grassland sites and six peatland sites (cf. supplementary material a, table S1 for details). Reference years with incomparable land use to 2018 (e.g. different crops in a crop rotation, or years before wood harvesting) were omitted and are already excluded from the above numbers.

While all radiation terms of equation (1.1) were measured directly and the turbulent fluxes were computed from high-frequency raw data [11-13], $S_l$ and $E_c$ were estimated according to:

$$E_c \approx -0.469 \frac{J}{\mu mol} NEE \tag{2.1}$$

and

$$S_l \approx SHF_d + d(\overline{\rho_s}\overline{c_s} + \overline{\theta_w}\rho_w\, c_w)\frac{\Delta\overline{T_s}}{\Delta t} + \frac{m_c}{A}\overline{c_c}\frac{\Delta\overline{T_c}}{\Delta t} + h_m\left(\overline{\rho_a}c_p\frac{\Delta\overline{T_a}}{\Delta t} + \lambda\frac{\Delta\overline{\rho_v}}{\Delta t}\right). \tag{2.2}$$

Note that in equation (2.1), past studies on energy balance closure (EBC) used different $CO_2$ flux components such as net ecosystem exchange (*NEE*), gross primary production (*GPP*) or overstorey $CO_2$ flux to estimate $E_c$, which typically contributes << 5% to the budget [14-18]. The measurement or modelling technique for the different components of $S_l$ (equation 2.2) determines whether heat released by respiration needs to be excluded, included or partly included in equation (2.1). In most cases including this study, the unknown fraction of (soil) respiration below level *d* (equation (2.2)) would need to be excluded. By estimating $E_c$ from *NEE*, we avoid overestimating energy balance closure and inducing further uncertainties from source partitioning. This also implies relative changes in $E_c$ reported in this study are equivalent to relative changes in net carbon uptake (ecosystem productivity) *NEP* = -*NEE*.

The soil heat flux at depth *d* ($SHF_d$) is measured by heat flux plates (first term on the right-hand side of equation (2.2)) and corrected for estimated storage changes over time ($\Delta/\Delta t$) between plate and soil surface (second term), in biomass (third term) and air below the flux measurement level (last term). They depend on temperature (*T*), density ($\rho$) and specific heat capacity (*c*) of the respective medium soil (*s*), soil water (*w*, $\theta_w$ being the volumetric soil water content), plant canopy (*c*, $m_c\, A^{-1}$ being wet biomass per unit area), air (*a*) and water vapour (*v*, $c_p$ being atmospheric heat capacity at constant pressure and $\lambda$ the water vaporisation enthalpy). In each term, the height integral was approximated by multiplying average available measurement values (indicated by overbars, see supplementary material (a) for details) with the respective layer thickness *d* and $h_m$ (height of flux level).

The combined inter-annual and spatial variability of the change of a variable in 2018 vs. the reference period was used to estimate its 95% confidence interval (more details in supplementary material a). We report only changes that were significant against this variability, unless explicitly stated otherwise.

For the water budget and drought intensity, the potential evapotranspiration (*ET* in absence of water stress) is an important characteristic, which can be estimated by the Penman-Monteith equation. To disentangle atmospheric conditions from site-specific responses and to rely on variables available with a high temporal coverage and quality at all sites, we used the grass reference evapotranspiration $ET_0$ [19]. A meteorological, atmospheric or potential drought is defined by either the anomaly in precipitation ($\Delta P$), or in the climatological water balance ($P - ET_0$) [20-22]. Obviously, the latter definition captures more of the processes that can eventually lead to actual drought stress or soil drought. However, not all of $ET_0$ leads to actual water loss by *ET* at each site, and $ET_0$ also correlates with factors positively affecting plant growth in energy-, temperature- or light-limited regions, such as $R_{si}$ or growing degree days. Therefore, Figures 1 and 2 depict all sites in a two-dimensional coordinate system of both $\Delta P$ and $\Delta ET_0$.

# Results and Discussion

### (a) Meteorological drought conditions

In 2018, most sites (46 of 56) were characterized by a joint negative ("dry") $\Delta P$, positive ("dry") $\Delta ET_0$, and $\Delta(P - ET_0)$ below -75 mm (lower right quadrant of figure 1a).

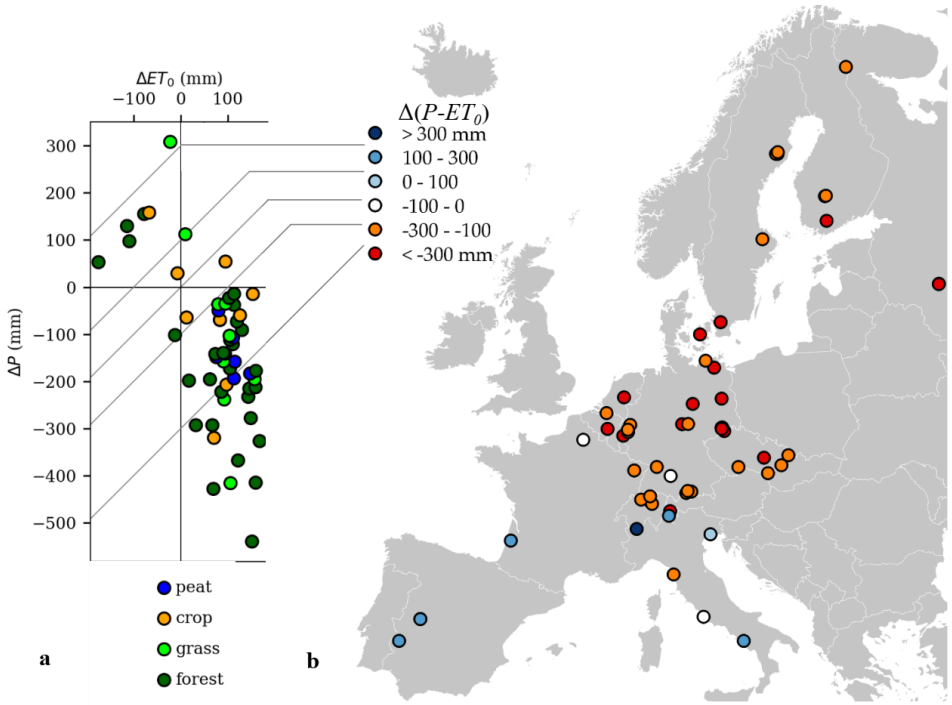


Figure 1: 2018 anomalies in precipitation ($P$) and grass reference evapotranspiration ($ET_0$); (a) by ecosystem type, diagonal broken lines correspond to $P$-$ET_0$ anomalies in steps of 100 mm; (b) by location, colours refer to bins of $P$-$ET_0$ anomalies.

This group of sites, which suffered atmospheric drought conditions according to any of these three definitions on an annual basis, will be referred to as *affected* sites. It includes 26 forest, seven crop, seven grassland and six peatland sites. While $\Delta P$ in this group spanned a large range of more than 500 mm, $\Delta ET_0$ was confined to a narrow band around +100 mm. On average, $P$ was reduced by 180 mm and $ET_0$ increased by 105 mm. Mean annual temperature across these sites was 0.82°C higher than in the reference period, with little variability among ecosystem types except for peatlands, which showed only 0.66 °C average increase and a comparatively large variability among sites (see supplementary material, table S2). The remaining smaller group of ten sites, referred to as *other*, included few sites with a moderate $\Delta(P - ET_0)$ deficit of less than 100 mm, and potential drought stress eminent only in $\Delta P$ or $\Delta ET_0$, but not both. The majority of this group, which may or may not have suffered drought conditions during subperiods of 2018, exhibited positive ("wet") annual $P$ anomalies jointly with negative ("wet") $ET_0$ anomalies. $\Delta ET_0$ was thus (negatively) correlated to $\Delta P$ (r = -0.60), and by its role in the Penman-Monteith equation positively to $R_{si}$ (r = 0.87), but also to the sum of growing degree days above 10°C (r = 0.78), which is potentially beneficial for plant growth. Flux site data thus confirm that over a large region of Europe, 2018 was not a singular rain-deficient, warm, or sunny year, but showed a combination of these anomalies. *Affected* sites were located in central Europe north of the Alps, Scandinavia and Eastern Europe (figure 1b), in general agreement with other ground-based and remote sensing observations as well as models [21, 23]. In particular, affected sites are well distributed across the region suffering the strongest annual reduction in the standardised precipitation-evapotranspiration index SPEI [24].

### (b) Changes in radiation balance and energy balance closure

Incoming shortwave (global solar) radiation ($R_{si}$) across *affected* sites increased by +360 MJ $m^{-2}$ $yr^{-1}$ (+9%), as opposed to -147 MJ $m^{-2}$ $yr^{-1}$ across the *other* sites. Radiation budget components other than $R_{si}$ were not available with sufficient coverage at all sites, such that the following results represent sub-datasets (see supplement table S2, minimum 35 *affected* and six *other* sites).

Outgoing shortwave radiation ($R_{so}$) was mostly following incoming radiation $R_{si}$, increasing slightly more (+11.5%), most likely due to a small net albedo change, which was however not significant, differing in sign between ecosystems and sites.

Incoming longwave radiation at *affected* sites changed insignificantly (+24 MJ $m^{-2}$ $yr^{-1}$,+0.2%, but +1.6% at *other* sites), indicating cancelling effects of increased atmosphere temperature (positive) and reduced cloudiness (negative). Outgoing longwave radiation, in contrast, reflected the higher land surface temperature at *affected* sites (148 MJ $m^{-2}$ $yr^{-1}$, +1.3%) in comparison to no significant change at *other* sites.

Net radiation ($R_n$) changed by +123 MJ $m^{-2}$ $yr^{-1}$ (+6.3%) across *affected* while not significantly across *other* sites, reflecting the dominant role of $R_{si}$ and the moderating role of higher outgoing longwave radiation from the warmer land surface. However, a large variability (95% confidence interval ±60 MJ $m^{-2}$ $yr^{-1}$) might indicate instrumental issues at some sites.

Eddy covariance measurements are known for a gap in the energy balance closure (EBC), i.e. the sum of $H$ and $\lambda ET$ is frequently 15 to 30% smaller than $R_n$- $S_l$-$E_c$ [25, 26]. Mean EBC across sites in this study changed by 3% between the reference period and 2018 (see supplementary material b for details), indicating that relative changes in the fluxes reported remain independent of the EBC problem. Due to the ongoing debate about its reasons and implications for any hypothetical flux correction, absolute fluxes are reported without any correction [27] for the EBC gap, which was on average 20% in our study.

### (c) Sensible heat and evapotranspiration

Among the non-radiative surface energy fluxes (left-hand side of equation 1.1), the sensible heat flux ($H$) showed the strongest and most consistent change across *affected* sites, with +169 MJ $m^{-2}$ $yr^{-1}$ (+32.3%, and no significant change across *other* sites, figure 2a).

Latent heat flux at *affected* sites did not change significantly on average (-0.3 MJ $m^{-2}$ $yr^{-1}$). We attribute this to the opposing roles of increased $ET_0$ on the one hand and soil water depletion, stomatal closure and plant development on the other hand. $ET$ increased where and when sufficient water was available from recent precipitation or from long-term storage, and later decreased only at sites where stored soil water was depleted (cf. supplementary material c). Consequently, among *affected* sites annual $\lambda ET$ typically decreased at those sites with a severe precipitation deficit, while it frequently increased at sites with the same $ET_0$ surplus but only moderate precipitation deficit (figure 2b). Figure 2c shows a clearer drought signal in the evaporative fraction (fraction of $H+\lambda ET$ used for $ET$): even where $ET$ increased, it typically increased less than proportionally to the larger energy available.

Averages across ecosystems further confirm this hypothesis of $ET$ response depending on stored water. *Affected* peatland sites were the only ecosystem type with a significant increase in $\lambda ET$ (+205 MJ $m^{-2}$ $yr^{-1}$) and no significant increase in $H$. Crop sites showed a significant decrease in $\lambda ET$ (-122 MJ $m^{-}$ $yr^{-1}$), which could have a number of reasons: i) Crop sites are under-represented among high elevation and high latitude sites, thus water limitation at a given precipitation deficit is more likely compared to some forest and grassland sites at higher elevations or latitudes; ii) crop sites typically feature periods of bare soil, during which $ET$ is

dominated by evaporation. Transpiration can be sustained longer than evaporation due to the access of plants roots to water in deeper soil layers; iii) these periods may start earlier in a drought year due to accelerated maturity and harvest (cf. supplementary material c).

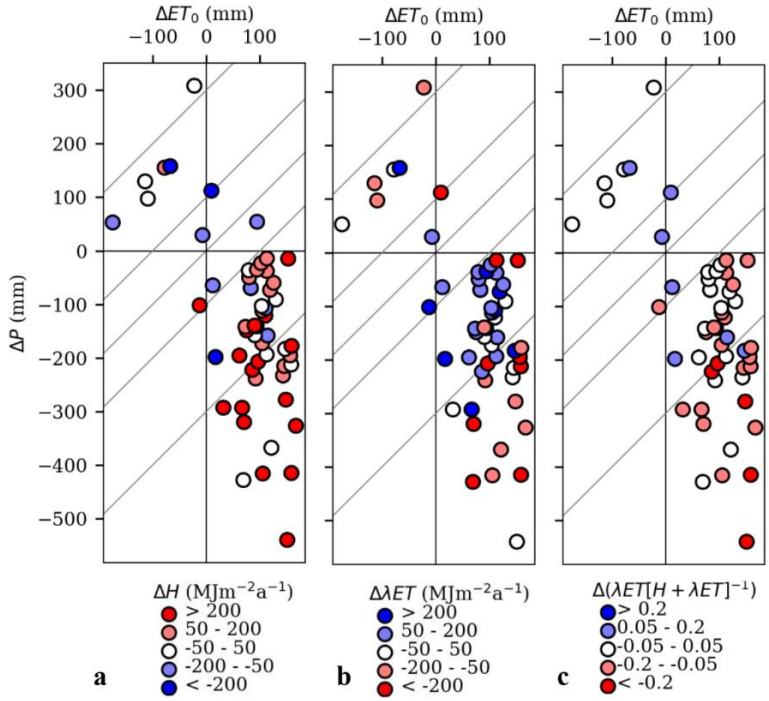


Figure 2: Annual 2018 anomalies of sensible heat flux (*H*) (a), latent heat flux (*λET*) (b), and evaporative fraction ($\lambda ET\,(H+\lambda ET)^{-1}$) (c) as a function of precipitation *P* and grass-reference $ET_0$ deficits. Diagonal isolines indicate $P$-$ET_0$ anomalies of 0, ±100, and ±300 mm (cf. figure 1).

In 2018, anomalies in *ET* of grassland, forest and *other* sites reacted to $ET_0$ and *P* as predicted by the Budyko framework ([28], figure 3).

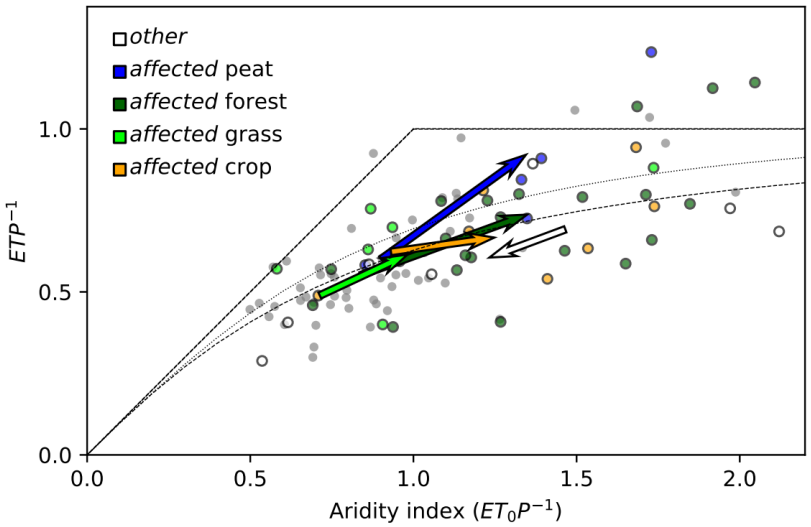


Figure 3: Budyko plot of the evaporative index ($ET\,P^{-1}$) vs. the aridity index ($ET_0\,P^{-1}$). Arrows show the mean shift of annual ratios between the reference period and 2018 (arrow head), averaged per affected ecosystem type and over all other sites. Circles indicate the ratios for each single site (coloured: in 2018, small grey: reference period, axes clipped due to maxima of $ET_0\,P^{-1}$ and $ET\,P^{-1}$ of 4.3 and 1.8, respectively). Dotted straight lines: Theoretical energy (1:1 line) and water (horizontal) limits; Grey line: Expected ensemble behaviour after [30]; broken line: Fit from [29] to FLUXNET data not corrected for energy balance closure.

A small offset may reflect a systematic underestimation of *ET* due to the EBC, and vanishes when comparing to the curve fit by Williams et al. [29]. At crop sites, however, the fraction of *P* used for *ET* increased less, as could be expected according to the above reasons. All six peatland sites showed an increase in *ET*, which was linearly related to the increase in $ET_0$. One of them (DE-SfS) is an ombrogenic bog fed only by precipitation, and showed the smallest *ET* increase and largest *H* increase among peatland sites. The remaining fen peatlands can receive additional inflows from the surrounding landscape and increase *ET* in response to higher $ET_0$ and lower *P* for a longer period than other ecosystems. Bogs show a vertical pore space structure and self-regulatory mechanisms [30] that could lead to an earlier decrease in *ET*. A few peatland and forest sites lost more water by *ET* than they received by *P* (points above the water limit line in figure 3). At one peatland site (DE-ZRK), available measurements of the change in water table depth between the start and the end of 2018 (-0.65 m) would reconcile $ET\,P_{2018}^{-1}$ (1.8, not shown in figure 3 for scaling reasons) with the theoretical water limit. A detailed analysis of the effect of extractable soil water in forests for selected sites is presented in [6].

On an annual basis, *affected* forest sites showed a larger average increase in *H* (+235 MJ $m^{-2}$ $yr^{-1}$) than grassland sites (+79 MJ $m^{-2}$ $yr^{-1}$), while the contrast in the insignificant *ET* changes between both ecosystems was opposite. For the case of 2003, it was demonstrated [7] that due to differences in stomatal control and rooting depth, forests show less *ET* and more *H* than grasslands during the early stage of a heatwave. Ultimately, however, the resulting more rapid depletion of available soil water under grass led to more atmospheric heating than over forests at the peak of the heatwave 2003 [7]. Evolutionary reasons for such a more conservative strategy of forests are suggested in [31]. According to our study, the former effect (more heating over forests) dominated over the latter (more heating over grasslands once soil water is depleted) on an annual basis in 2018. This may be partly due to the lower albedo and resulting higher total available energy of forests, partly due to the grassland ensemble including more humid sites (see figure 3), and partly to the different timescales of the studies. A brief sub-annual comparison between grasslands and forests largely supporting [7] is presented in supplementary material c. Also for 2003, an analysis of four example catchments showed a net increase of *ET* [32] to amplify the soil drought, which could not be found at the majority of our sites on an annual basis in 2018. However, as a consequence of more available energy transferred as *H*, apart from direct heating of the atmosphere, precipitation can also be reduced due to a higher and cooler cloud base [33].

### (d) Minor energy fluxes, water-use efficiency of $CO_2$ uptake, and soil water content

The increase in heat storage in the soil and the canopy was small (+9 MJ $m^{-2}$ $yr^{-1}$ across *affected* sites), demonstrating that most of the additional energy during a warm and dry anomaly is transferred back to the atmosphere. Relative change was large (~300%) due to the fact that net energy storage was approximately balanced in the reference period.

The change in energy storage in photosynthesis products was even smaller, and highly variable between sites (-1.6 MJ $m^{-2}$ $yr^{-1}$ across *affected*, insignificant across *other* sites). However, the change across *affected* sites corresponds to 17.8% of reference period $CO_2$ uptake, or 38 g C $m^{-2}$ $yr^{-1}$. The radiative forcing of this amount not removed from the atmosphere in 2018, estimated according to the methodology of [34] and [35], corresponds to 1.9 MJ $m^{-2}$ $yr^{-1}$ during each year of its atmospheric lifetime, such that the total heating effect due to unused photosynthetic energy and the greenhouse effect cumulates to, e.g., 3.5 MJ $m^{-2}$ $yr^{-1}$ in 2019. Our observation of a reduced net $CO_2$ uptake across *affected* sites is in general agreement with observed changes in atmospheric $CO_2$ concentrations over Europe [36, 37].

$CO_2$ uptake is typically closely related to *ET* loss through the concept of water-use efficiency [40, 41]. Inherent water use efficiency (IWUE*) estimated from annual *GPP*, vapour pressure deficit and *ET* according to Beer et al. [40] increased across *affected* sites by 3.1 g C hPa $kg^{-1}$ $H_2O$ (31.4%, no significant change across *other* sites). For assessing the climatological response of the land surface to drought, it is worthwhile to also consider the net ecosystem water use efficiency $-NEE\ ET^{-1}$ (WUEeco) or, dimensionless, $E_c\ \lambda ET^{-1}$. While $CO_2$ uptake adds to the potential of an ecosystem to mitigate drought and heat waves in any respect (see above), *ET* has ambiguous effects, providing a local cooling and moistening of the atmosphere on the one hand, while on the other hand transferring latent heat to the atmosphere, adding $H_2O$ to its greenhouse gas concentration at least on a short term, and depleting soil water needed for future productivity. $E_c\ \lambda ET^{-1}$ decreased across *affected* sites by $-11 \cdot 10^{-4}$ (-13.8%, no significant change across *other* sites). On average, the affected land surface thus reinforced water scarcity and global warming during the drought and heat wave. Soil water content measured within the top 0.3 m of the soil decreased on average by -0.05 $cm^3\ cm^{-3}$ (-16.2%), while increasing by 0.03 $cm^3\ cm^{-3}$ across *other* sites. Differences between forest and grassland sites in both IWUE* and WUEeco (table S2) are in qualitative agreement with a forest – grassland comparison among Swiss sites, where forest significantly increased water use efficiency [31]. However, figure 4 demonstrates that the relation between smaller $CO_2$ uptake and increased *ET* water loss [2], was not universal.

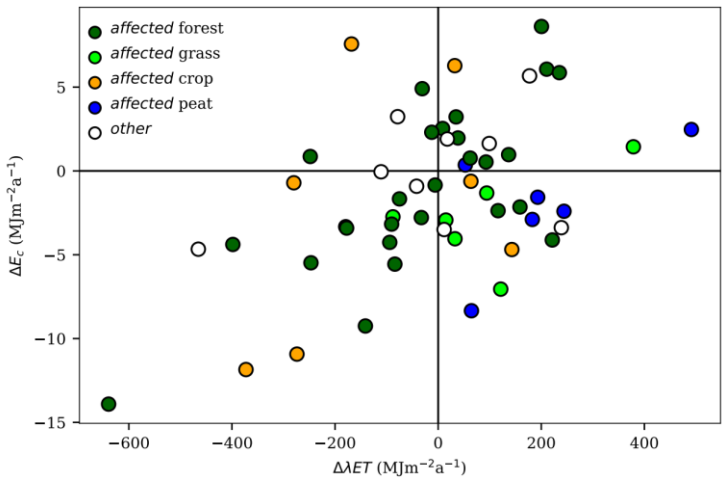


Figure 4: 2018 annual anomalies in energy used for $CO_2$ uptake ($E_c$), vs. energy used for evapotranspiration ($\lambda ET$) (r = 0.49, reduced major axis slope = 0.023).

Peatlands typically lost more water via *ET* than in the reference period without absorbing more $CO_2$, possibly because of exposure of large amounts of organic carbon in otherwise inundated soils to aerobic conditions favouring respiration, or an increase in evaporation rather than transpiration. Some of the *affected* cropland and forest sites, in contrast, showed increased $CO_2$ uptake with no or little additional water loss. A more detailed future analysis of the site-specific conditions causing such responses might help to develop more drought- and warming-resilient land-use strategies.

# Conclusions

Among the land surface responses to the 2018 European drought, a considerable relative increase in sensible heat flux (*H*) by 32.3% was the most important change in absolute terms, as well as the most consistent one across ecosystem types and drought intensities. Latent heat flux ($\lambda ET$) did not change significantly on average but showed a large variability, including

increases at sites with large water reservoirs (peatlands) or moderate drought intensity and stronger decreases at crop sites. However, the evaporative fraction (fraction of turbulent heat transfer used for $\lambda ET$) clearly decreased and the evaporative index (fraction of precipitation used for $\lambda ET$) clearly increased across ecosystems. Responses in energy used for net $CO_2$ uptake ($E_c$) showed a correspondingly large variability and a moderate correlation to $\lambda ET$ response, but a significant average decrease of -17.8%. Heat storage in the ground showed a strong relative but small absolute increase, and the response of albedo was variable, generally small and as a result not significant across the assessed sites.

Albedo and $E_c$ potentially cool the land surface – atmosphere system, the latter both through energy consumption during photosynthesis and greenhouse gas removal, while $H$ has a heating effect. $\lambda ET$ has a large variety of effects including local cooling and nonlocal heating of the atmosphere, atmospheric humidity and cloud formation, and depletion of water resources required for productivity and groundwater recharge. Thus an increase or decrease in $ET$ does not generally mitigate or reinforce drought, but must be assessed considering local priorities and potential correlations with $E_c$ and albedo. Since $H$ increased consistently, $CO_2$ uptake decreased on average, and albedo and $ET$ showed no consistent change, the affected European land surface responded with a clear net heating effect to the drought in 2018.

## Data accessibility

This study is mainly based on the dataset: https://doi.org/10.18160/YVR0-4898. Data of additional sites and missing single variables for some sites have been obtained directly from the institutions and are available from the data repositories of these institutions. The corresponding author can provide the respective institutional contact or repository on request.

## Author contributions

A.G., A.Kl., C.Br., C.R., F.S. and H.V. conceived the study. A.G. and A.Kl. assembled the database, designed the scripts and figures, and carried out the analysis, with input from all other authors. A.G. wrote the manuscript with input from all authors. All authors read, corrected and approved the submitted version of the manuscript. Analysis of raw data from each site towards half-hourly averages and fluxes, planning and quality assurance of the sites was provided by all authors. Competing interests. We declare we have no competing interests.

## Funding

Authors thank the funders (grant IDs and particularly concerned authors/sites in parentheses) French National Research Agency ANR (ANR-11-LABX-0002-01, ANR-16-SUMF-0001-01, LabEx ARBRE, M.C.), Alexander von Humbold Stiftung (MaNiP, T.S.E.-M., M.Mi.), German Federal Ministry of Education and Research BMBF (01LN1313A, A.G.; ICOS; DE-Geb), German Federal Ministry of Food and Agriculture BMEL (ERA-NET FACCE ERAGAS, P.G., F.S., C.Br.), German Research Foundation DFG (BE1721/23, C.Be., T.G., DE-Tha; PAK 346; FOR 1695, A.P., J.I., H.W., DE-EC2, DE-EC4; INST 186/1118-1 FUGG, A.Kn., L.S.), GIP Ecofor SOERE F-ORE-T (M.C.), Finnish Center of Excellence (307331, I.M.), Research Foundation-Flanders FWO (BE-Bra; G0H3317N, B.G.), Hainich National Park (DE-Hai), Helmholtz Association HGF (TERENO; VH-NG-821, T.S.), Horizon 2020 (696356, P.G.), ICOS-FINLAND (281255, I.M.), Kempe Foundation (SMK-1743, J.C.), Knut and Alice Wallenberg Foundation (2015.0047, M.P.), Max-Planck Institute for Biogeochemistry (DE-Geb), Russian Foundation for Basic Research RFBR (19-04-01234-a, A.V.), Swiss National Science Foundation (ICOS-CH Phase 2 20FI20_173691, M.G., N.Bu.; InnoFarm 407340_172433, N.Bu.), European Commission (SUPER-G, S.G.; RINGO, L.H.; ERA-NET Sumforest No. 606803, M.C.), Service Public de Wallonie (DGO6, 1217769, A.D.L., B.H., B.L., C.V.), SustES (CZ.02.1.01/0.0/0.0/16_019/0000797, L.Š., M.F.), CzeCOS (grant no. LM2015061, L.F., L.Š., M.F., N.K.), Swedish Research Council FORMAS (2016-01289, M.P.; 942-2015-49, J.C.) and University of Padua (CDPA148553, 2014, A.Pi.)

## Acknowledgements

The authors thank all site collaborators, the Drought 2018 Task Force and the Ecosystem Thematic Centre of the ICOS Research Infrastructure for data provision, as well as two anonymous referees and guest editor W. Kutsch for suggestions that greatly helped to improve the manuscript, and senior editor Helen Eaton for multiple support during the revision and publication process.

## References

[1] Ciais, P., Reichstein, M., Viovy, N., Granier, A., Ogee, J., Allard, V., Aubinet, M., Buchmann, N., Bernhofer, C., Carrara, A., et al. 2005 Europe-wide reduction in primary productivity caused by the heat and drought in 2003. *Nature* **437**, 529-533.

[2] Reichstein, M., Ciais, P., Papale, D., Valentini, R., Running, S., Viovy, N., Cramer, W., Granier, A., Ogee, J., Allard, V., et al. 2007 Reduction of ecosystem productivity and respiration during the European summer 2003 climate anomaly: a joint flux tower, remote sensing and modelling analysis. *Global Change Biology* **13**, 634-651.

[3] Lorenzini, G., Nali, C. & Pellegrini, E. 2014 Summer heat waves, agriculture, forestry and related issues: an introduction (Editorial). *Agrochimica* **58**, 3-19.

[4] Copernicus Climate Change Service. 2019 European State of the Climate 2018 (https://climate.copernicus.eu/ESOTC/2018).

[5] Copernicus Climate Change Service. 2020 European State of the Climate 2019 (https://climate.copernicus.eu/ESOTC/2019).

[6] Gourlez de la Motte, L., Beauclaire, Q., Heinesch, B., Longdoz, B. & al., e. submitted Stomatal and non-stomatal limitations of gross primary productivity in forest ecosystems during edaphic drought. *Philosophical Transactions of the Royal Society B*, **this issue**.

[7] Teuling, A. J., Seneviratne, S. I., Stockli, R., Reichstein, M., Moors, E., Ciais, P., Luyssaert, S., van den Hurk, B., Ammann, C., Bernhofer, C., et al. 2010 Contrasting response of European forest and grassland energy exchange to heatwaves. *Nat. Geosci.* **3**, 722-727. (DOI:10.1038/ngeo950).

[8] Swinbank, W. C. 1951 The measurement of vertical transfer of heat and water vapor by eddies in the lower atmosphere. *Journal of Meteorology* **8**, 135-145. (DOI:10.1175/1520-0469(1951)008<0135:tmovto>2.0.co;2).

[9] Drought 2018 Team and ICOS Ecosystem Thematic Centre 2020: Drought-2018 ecosystem eddy covariance flux product for 52 stations in FLUXNET-Archive format, doi:10.18160/YVR0-4898 (https://www.icos-cp.eu/).

[10] Franz, D. & Acosta, M. & Altimir, N. & Arriga, N. & Arrouays, D. & Aubinet, M. & Aurela, M. & Ayres, E. & Lopez-Ballesteros, A. & Barbaste, M., et al. 2018 Towards long-term standardised carbon and greenhouse gas observations for monitoring Europe's terrestrial ecosystems: a review. *Int. Agrophys.* **32**, 439-+. (DOI:10.1515/intag-2017-0039).

[11] Mauder, M., Cuntz, M., Drüe, C., Graf, A., Rebmann, C., Schmid, H.-P., Schmidt, M. & Steinbrecher, R. 2013 A quality assessment strategy for long-term eddy-covariance measurements. *Agric. For. Meteorol.* **169**, 122-135.

[12] Sabbatini, S., Mammarella, I., Arriga, N., Fratini, G., Graf, A., Hortriagl, L., Ibrom, A., Longdoz, B., Mauder, M., Merbold, L., et al. 2018 Eddy covariance raw data processing for CO2 and energy fluxes calculation at ICOS ecosystem stations. *Int. Agrophys.* **32**, 495-+. (DOI:10.1515/intag-2017-0043).

[13] Wutzler, T., Lucas-Moffat, A., Migliavacca, M., Knauer, J., Sickel, K., Sigut, L., Menzer, O. & Reichstein, M. 2018 Basic and extensible post-processing of eddy covariance flux data with REddyProc. *Biogeosciences* **15**, 5015-5030. (DOI:10.5194/bg-15-5015-2018).

[14] Blanken, P. D., Black, T. A., Yang, P. C., Neumann, H. H., Nesic, Z., Staebler, R., den Hartog, G., Novak, M. D. & Lee, X. 1997 Energy balance and canopy conductance of a boreal aspen forest: Partitioning overstory and understory components. *Journal of Geophysical Research-Atmospheres* **102**, 28915-28927. (DOI:10.1029/97jd00193).

[15] Meyers, T. P. & Hollinger, S. E. 2004 An assessment of storage terms in the surface energy balance of maize and soybean. *Agric. For. Meteorol.* **125**, 105-115. (DOI:10.1016/j.agrformet.2004.03.001).

[16] Eshonkulov, R., Poyda, A., Ingwersen, J., Wizemann, H. D., Weber, T. K. D., Kremer, P., Hogy, P., Pulatov, A. & Streck, T. 2019 Evaluating multi-year, multi-site data on the energy balance closure of eddy-covariance flux measurements at cropland sites in southwestern Germany. *Biogeosciences* **16**, 521-540. (DOI:10.5194/bg-16-521-2019).

[17] Oncley, S. P., Foken, T., Vogt, R., Kohsiek, W., DeBruin, H. A. R., Bernhofer, C., Christen, A., van Gorsel, E., Grantz, D., Feigenwinter, C., et al. 2007 The Energy Balance Experiment EBEX-2000. Part I: Overview and energy balance. *Bound.-Layer Meteor.* **123**, 1-28.

[18] Leuning, R., van Gorsel, E., Massman, W. J. & Isaac, P. R. 2012 Reflections on the surface energy imbalance problem. *Agric. For. Meteorol.* **156**, 65-74.

[19] Allen, R. G., Pereira, L. S., Raes, D. & Smith, M. 1998 *Crop evapotranspiration: Guidelines for computing crop water requirements*. Rome, FAO; 300 p.

[20] Thornthwaite, C. W. 1948 An Approach toward a Rational Classification of Climate. *Geographical Review* **38**, 55-94. (DOI:10.2307/210739).

[21] Buras, A., Rammig, A. & Zang, C. S. 2019 Quantifying impacts of the drought 2018 on European ecosystems in comparison to 2003. *Biogeosciences Discuss.* **2019**, 1-23. (DOI:10.5194/bg-2019-286).

[22] Vicente-Serrano, S. M., Begueria, S., Lorenzo-Lacruz, J., Camarero, J. J., Lopez-Moreno, J. I., Azorin-Molina, C., Revuelto, J., Moran-Tejeda, E. & Sanchez-Lorenzo, A. 2012 Performance of Drought Indices for Ecological, Agricultural, and Hydrological Applications. *Earth Interact.* **16**, 27. (DOI:10.1175/2012ei000434.1).

[23] Bastos, A., Ciais, P., Friedlingstein, P., Sitch, S., Pongratz, J., Fan, L., Wigneron, J. P., Weber, U., Reichstein, M., Fu, Z., et al. submitted Direct and seasonal legacy effects of the 2018 heat and drought on European ecosystem productivity. *Science Advances* 6, eaba2724 (doi:10.1126/sciadv.aba2724).

[24] Vicente-Serrano, S. M. & Begueria, S. 2020 SPEI Global Drought Monitor (https://spei.csic.es/map/maps.html).

[25] Stoy, P. C., Mauder, M., Foken, T., Marcolla, B., Boegh, E., Ibrom, A., Arain, M. A., Arneth, A., Aurela, M., Bernhofer, C., et al. 2013 A data-driven analysis of energy balance closure across FLUXNET research sites: The role of landscape scale heterogeneity. *Agric. For. Meteorol.* **171-172**, 137-152. (DOI:https://doi.org/10.1016/j.agrformet.2012.11.004).

[26] Wilson, K., Goldstein, A., Falge, E., Aubinet, M., Baldocchi, D., Berbigier, P., Bernhofer, C., Ceulemans, R., Dolman, H., Field, C., et al. 2002 Energy balance closure at FLUXNET sites. *Agric. For. Meteorol.* **113**, 223-243. (DOI:10.1016/s0168-1923(02)00109-0).

[27] Foken, T., Aubinet, M., Finnigan, J. J., Leclerc, M. Y., Mauder, M. & U, K. T. P. 2011 Results of a Panel Discussion About the Energy Balance Closure Correction for Trace Gases. *Bulletin of the American Meteorological Society* **92**, ES13-ES18.

[28] Budyko, M. I. 1974 *Climate and Life*, Academic Press.

[29] Williams, C. A., Reichstein, M., Buchmann, N., Baldocchi, D., Beer, C., Schwalm, C., Wohlfahrt, G., Hasler, N., Bernhofer, C., Foken, T., et al. 2012 Climate and vegetation controls on the surface water balance: Synthesis of evapotranspiration measured across a global network of flux towers. *Water Resources Research* **48**, W06523 (DOI:10.1029/2011wr011586).

[30] Nijp, J. J., Metselaar, K., Limpens, J., Bartholomeus, H. M., Nilsson, M. B., Berendse, F. & van der Zee, S. 2019 High-resolution peat volume change in a northern peatland: Spatial variability, main drivers, and impact on ecohydrology. *Ecohydrology* **12**, 17. (DOI:10.1002/eco.2114).

[31] Wolf, S., Eugster, W., Ammann, C., Hani, M., Zielis, S., Hiller, R., Stieger, J., Imer, D., Merbold, L. & Buchmann, N. 2013 Contrasting response of grassland versus forest carbon and water fluxes to spring drought in Switzerland. *Environ. Res. Lett.* **8**, 12. (DOI:10.1088/1748-9326/8/3/035007).

[32] Teuling, A. J., Van Loon, A. F., Seneviratne, S. I., Lehner, I., Aubinet, M., Heinesch, B., Bernhofer, C., Grunwald, T., Prasse, H. & Spank, U. 2013 Evapotranspiration amplifies European summer drought. *Geophys. Res. Lett.* **40**, 2071-2075. (DOI:10.1002/grl.50495).

[33] Kabat, P., Claussen, M., Dirmeyer, P., Gash, J. H. C., Bravo de Guenni, L., Meybeck, M., Pielke Sr, R., Vörösmarty, C. J., Hutjes, R. & Lütkemeier, S. 2004 *Vegetation, Water, Humans and the Climate: A New Perspective on an Interactive System*. Dordrecht, The Netherlands: Springer.

[34] Betts, R. A. 2000 Offset of the potential carbon sink from boreal forestation by decreases in surface albedo. *Nature* **408**, 187-190. (DOI:10.1038/35041545).

[35] Rotenberg, E. & Yakir, D. 2010 Contribution of Semi-Arid Forests to the Climate System. *Science* **327**, 451-454. (DOI:10.1126/science.1179998).

[36] Ramonet, M., Ciais, P., Apadula, F., Bastos, A., Bergamaschi, P., Blanc, P. E., Brunner, D., Caracciolo di Torchiaro, L., Calzolari, F., Chen, H., et al. submitted The fingerprint of the summer 2018 drought in Europe on ground-based atmsopheric CO2 measurements. *Philosophical Transactions of the Royal Society B*, **this issue**.

[37] Thompson, R. L., Broquet, G., Gerbig, C., Koch, T., Lang, M., Monteil, G., Munassar, S., Nickless, A., Scholze, M., Ramonet, M., et al. submitted Changes in Net Ecosystem Exchange over Europe During the 2018 Drought Based on Atmsopheric Observations. *Philosophical Transactions of the Royal Society B*, **this issue**.

[38] Wohlfahrt, G., Gerdel, K., Migliavacca, M., Rotenberg, E., Tatarinov, F., Muller, J., Hammerle, A., Julitta, T., Spielmann, F. M. & Yakir, D. 2018 Sun-induced fluorescence and gross primary productivity during a heat wave. *Sci Rep* **8**, 9. (DOI:10.1038/s41598-018-32602-z).

[39] Stoy, P. C., El-Madany, T. S., Fisher, J. B., Gentine, P., Gerken, T., Good, S. P., Klosterhalfen, A., Liu, S. G., Miralles, D. G., Perez-Priego, O., et al. 2019 Reviews and syntheses: Turning the challenges of partitioning ecosystem evaporation and transpiration into opportunities. *Biogeosciences* **16**, 3747-3775. (DOI:10.5194/bg-16-3747-2019).

[40] Beer, C., Ciais, P., Reichstein, M., Baldocchi, D., Law, B. E., Papale, D., Soussana, J. F., Ammann, C., Buchmann, N., Frank, D., et al. 2009 Temporal and among-site variability of inherent water use efficiency at the ecosystem level. *Global Biogeochemical Cycles* **23**, 13. (DOI:10.1029/2008gb003233).

# Supplementary material

*Table S1: Overview of sites used in this study. Longitude (Lon), Latitude (Lat), long-term mean annual temperature (MAT) and precipitation (MAP) are according to the European Fluxes Database cluster (http://www.europe-fluxdata.eu) for sites in this database, and provided by site PIs accordingly otherwise. Ecosystem refers to the simplified Four-type classification used in this study. Reference years from within the period 2004-2017 were chosen based on data availability and, in case of crop rotation sites, the same crop being grown as in 2018.*

| Site | Lon | Lat | IGBP | MAT (°C) | MAP (mm) | Elevation (m) | Ecosystem | Reference years | Reference |
|---|---|---|---|---|---|---|---|---|---|
| BE-Bra | 4.5 | 51.3 | MF | 9.8 | 750 | 16 | forest | 2004-2017 | [1] |
| BE-Lon | 4.7 | 50.6 | CRO | 10 | 800 | 167 | crop | 2006, 10, 14 | [2] |
| BE-Vie | 6.0 | 50.3 | MF | 7.8 | 1062 | 493 | forest | 2004-2017 | [3] |
| CH-Aws | 9.8 | 46.6 | GRA | 2.3 | 918 | 1978 | grass | 2011, 2016,2017 | [4] |
| CH-Cha | 8.4 | 47.2 | GRA | 9.5 | 1136 | 400 | grass | 2006-2017 | [5] |
| CH-Dav | 9.9 | 46.8 | ENF | 3.5 | 1046 | 1639 | forest | 2004-2017 | [6] |
| CH-Fru | 8.5 | 47.1 | GRA | 7.2 | 1651 | 982 | grass | 2006-2017 | [4] |
| CH-Lae | 8.4 | 47.5 | MF | 8.7 | 1211 | 689 | forest | 2005-2017 | [6] |
| CH-Oe2 | 7.7 | 47.3 | CRO | 9.8 | 1155 | 452 | crop | 2008, 2013 | [7] |
| CZ-BK1 | 18.5 | 49.5 | ENF | 6.7 | 1316 | 875 | forest | 2015-2017 | [8] |
| CZ-Lnz | 16.9 | 48.7 | MF | 9.3 | 550 | 150 | forest | 2016-2017 | [9] |
| CZ-RAJ | 16.7 | 49.4 | ENF | 7.1 | 681 | 625 | forest | 2013-2017 | [10] |
| CZ-Stn | 18.0 | 49.0 | DBF | 8.7 | 685 | 550 | forest | 2015-2017 | [11] |
| CZ-wet | 14.8 | 49.0 | WET | 7.7 | 604 | 425 | peatland | 2007-2017 | [12] |
| DE-BER | 13.3 | 52.2 | URB | 9.4 | 525 | 61 | grass | 2016-2017 | [13] |
| DE-EC2 | 8.7 | 48.9 | CRO | 9.4 | 889 | 318 | crop | 2011, 13, 15, 17 | [14] |
| DE-EC4 | 9.8 | 48.5 | CRO | 7.5 | 1064 | 687 | crop | 2011, 14, 15 | [15] |
| DE-Fen | 11.1 | 47.8 | GRA | 8.4 | 1081 | 595 | grass | 2012- 2017 | [16] |
| DE-Geb | 10.9 | 51.1 | CRO | 8.5 | 470 | 162 | crop | 2007, 08, 10, 14, 16 | [17] |
| DE-Gri | 13.5 | 51.0 | GRA | 7.8 | 901 | 385 | grass | 2005-2017 | [18] |
| DE-Hai | 10.5 | 51.1 | DBF | 8.3 | 720 | 440 | forest | 2004-2017 | [19] |
| DE-HoH | 11.2 | 52.1 | DBF | 9.1 | 563 | 193 | forest | 2015-2017 | [20] |
| DE-Hte | 12.2 | 54.2 | WET | 9.2 | 645 | 0 | peatland | 2016-2017 | [21] |
| DE-Kli | 13.5 | 50.9 | CRO | 7.6 | 842 | 478 | crop | 2007, 2012 | [18] |
| DE-Obe | 13.7 | 50.8 | ENF | 5.5 | 996 | 734 | forest | 2009-2017 | [18] |
| DE-RbW | 11.0 | 47.7 | GRA | 9.0 | 1160 | 769 | grass | 2012-2017 | [16] |
| DE-RuR | 6.3 | 50.6 | GRA | 7.7 | 1033 | 515 | grass | 2012-2017 | [22] |
| DE-RuS | 6.4 | 50.9 | CRO | 10.2 | 718 | 103 | crop | 2013, 2015 | [23]. |
| DE-RuW | 6.3 | 50.5 | ENF | 7.5 | 1250 | 610 | forest | 2014-2017 | [24] |
| DE-SfS | 11.3 | 47.8 | WET | 8.6 | 1127 | 590 | peatland | 2013-2017 | [25] |
| DE-Tha | 13.6 | 51.0 | ENF | 8.2 | 843 | 380 | forest | 2004-2017 | [18] |
| DE-ZRK | 12.9 | 53.9 | WET | 8.7 | 584 | 1 | peatland | 2016-2017 | [26] |
| DK-Sor | 11.6 | 55.5 | DBF | 8.2 | 660 | 40 | forest | 2004-2017 | [27] |
| ES-Abr | -6.8 | 38.7 | SAV | 16 | 400 | 280 | forest | 2016-2017 | [28] |
| ES-LM1 | -5.8 | 39.9 | SAV | 16 | 700 | 265 | forest | 2016-2017 | [29] |
| ES-LM2 | -5.8 | 39.9 | SAV | 16 | 700 | 270 | forest | 2016-2017 | [29] |
| FI-Hyy | 24.3 | 61.8 | ENF | 3.8 | 709 | 180 | forest | 2004-2017 | [30] |
| FI-Let | 24.0 | 60.6 | ENF | 4.6 | 627 | 0 | forest | 2017 | [31] |
| FI-Sii | 24.2 | 61.8 | WET | 3.5 | 701 | 160 | peatland | 2016-2017 | [32] |
| FI-Var | 29.6 | 67.8 | ENF | -0.5 | 601 | 395 | forest | 2017-2017 | [33] |
| FR-Bil | -1.0 | 44.5 | ENF | 12.8 | 930 | 0 | forest | 2015-2017 | [34] |
| FR-EM2 | 3.0 | 49.9 | CRO | 10.8 | 680 | 84 | crop | 2015, 2018 | [35] |
| FR-Hes | 7.1 | 48.7 | DBF | 9.2 | 820 | 300 | forest | 2014-2017 | [36] |
| IT-BCi | 15.0 | 40.5 | CRO | 18 | 600 | 15 | crop | 2017 | [37] |
| IT-Cp2 | 12.4 | 41.7 | EBF | 15.2 | 805 | 6 | forest | 2013-2017 | [38] |
| IT-Lsn | 12.8 | 45.7 | OSH | 13.1 | 1083 | 1 | crop | 2017-2017 | [39] |
| IT-SR2 | 10.3 | 43.7 | ENF | 14.2 | 920 | 4 | forest | 2014-2017 | [40] |
| IT-Tor | 7.6 | 45.8 | GRA | 2.9 | 920 | 2160 | grass | 2009-2017 | [41] |
| NL-Loo | 5.7 | 52.2 | ENF | 9.8 | 786 | 25 | forest | 2004-2017 | [42] |
| RU-Fy2 | 32.9 | 56.4 | ENF | 3.9 | 711 | 265 | forest | 2016-2017 | [43] |
| RU-Fyo | 32.9 | 56.5 | ENF | 3.9 | 711 | 265 | forest | 2016-2017 | [44] |
| SE-Deg | 19.6 | 64.2 | WET | 1.2 | 523 | 270 | peatland | 2015-2017 | [45] |
| SE-Htm | 13.4 | 56.1 | ENF | 7.4 | 707 | 115 | forest | 2016-2017 | [46] |
| SE-Nor | 17.5 | 60.1 | ENF | 5.5 | 527 | 46 | forest | 2014-2017 | [47] |
| SE-Ros | 19.7 | 64.2 | ENF | 1.8 | 614 | 160 | forest | 2015-2017 | [48] |
| SE-Svb | 19.8 | 64.3 | ENF | 1.8 | 614 | 270 | forest | 2015-2016 | [49] |

## (a) Data processing methods

An overview of sites is given in table S1. Raw data measured at 10 or 20 $s^{-1}$ were processed towards half-hourly fluxes by each single site operator. Data gaps in fluxes and meteorological time series were filled, and *GPP* estimated, according to [50-55]. For sites where raw fluxes were directly provided within this study, these steps were performed by the authors, including a neighbour-based gap-filling of meteorological data between close sites [54]. For most sites, provided through the European Fluxes database cluster (http://www.europe-fluxdata.eu/), processing was performed by the Ecosystem Thematic Centre of ICOS RI and the intermediate result published [56]. Due to a slightly better performance on longer gaps than the marginal distribution sampling method implemented in [55], gaps in $\lambda ET$ were filled by regression through the origin against $ET_0$, using an adaptive window as described in [53]. Subsequently the remaining available energy according to $ET_0$ was used in the same way to fill gaps in $H$. A site was used if after these steps turbulent fluxes of sensible and latent heat and $CO_2$ as well as incoming solar radiation, air temperature, humidity and precipitation were available for at least 80% of the period April to September and at least 60% of the full year, both for 2018 and at least one year in the period from 2004 to 2017. Data of the available years from this period were averaged to serve as a reference, with an additional constraint of omitting years with incomparable land use conditions (e.g. different crops in a crop rotation, or the years before wood harvesting). Remaining gaps in final variables required as an unbiased annual budget were filled by first applying reduced major axis [57] regression between the daily time series of 2018 and the reference year and finally, if required, linear regression. Statistics that do not require gapless annual budgets, but a list of jointly available variables, such as energy balance closure EBC [58], were computed without this step after list-wise deletion of input records with missing data. In equation (2.2), due to varying data availability between sites, we used site-specific values of $d$ and $h_m$, but a global estimate of 1.42 $10^6$ J $m^{-3}$ $K^{-1}$ for $\rho_s c_s$. $T_c$ was in most cases approximated by $T_a$; $m_c A^{-1}$ was either known for a site or approximated from canopy height $h_c$ via regression on all sites with known $h_c$ and $m_c A^{-1}$. Grass reference evapotranspiration according to [59] was computed using the hourly version with solar incoming radiation ($R_{si}$). The sum parameter of growing-degree days was computed by cumulatively adding all mean daily temperatures above 10°C per year.

To estimate confidence intervals of changes in fluxes and state variables across groups of sites (i.e. *affected* ecosystems or the group of all *affected* vs. all *other* sites), we considered both, the inter-annual variability between multiple reference years at each sites, and the spatial variability between sites in the same group. Systematic measurement errors were not included given that they likely affect all years similarly, in line with [60], which is explicitly shown for the energy balance closure gap in the following section. Random errors in half-hourly measurements [61] strongly decrease in relative importance during propagation into annual sums [60]. For those sites and variables where estimates on annually aggregated random errors were available [56, 62], these were considerably smaller than the measured inter-annual variability, in which they are implicitly included. The mean change across a group of sites, for each of which a mean reference year was computed beforehand, is equivalent to a weighted average of differences between 2018 and each single reference year, where the weights are the inverse of the number of reference years available for the site. The corresponding confidence interval is given by

$$\mathrm{CI} = x \pm t_{\left(1-\frac{\alpha}{2}, N_{eff}-1\right)} \sqrt{\frac{\overline{s_{ia}{}^2} + s_{sp}{}^2}{N_{eff}-1}}, \qquad \text{(S1)}$$

where CI is the two-sided confidence interval of the change x at error probability α (0.05 for the 95% confidence), $t$ student's t distribution, $s_{ia}{}^2$ the biased (uncorrected) inter-annual variance among reference years at each site, $s_{sp}{}^2$ the biased spatial variance of mean changes between the sites of the group, and the overbar denotes averaging. Note that the root term is the standard error and its product

with $\sqrt{N_{eff}}$ the unbiased standard deviation. $N_{eff}$ is the effective sample size of a weighted variance [63], which is in our case exactly equivalent to

$$N_{eff} = \frac{1}{\left(\frac{1}{N_{ia}}\right)} \cdot N_{sp}. \quad \text{(S2)}$$

The first factor is the harmonic mean of the number of reference years available at the sites in the group, the second the number of sites. Confidence intervals not including zero indicate a significant change. Mean and relative changes, their confidence interval, and number of sites with available measurements of the respective variable are given in table S2. The same approach is used in figure S2 to estimate confidence intervals from the combined variances between days in a rolling window, reference years and sites. In this case, the number of days in the rolling window contributing to $N_{\mathrm{eff}}$ could lead to erroneously narrow confidence intervals due to correlation (dependence) between consecutive days. Following autocorrelation analyses of daily flux data, we thus reduced the number of days contributing to $N_{\mathrm{eff}}$ by a factor of four days to arrive at conservative confidence interval estimates.

*Table S2: Overview of absolute and relative changes of discussed variables in 2018 vs. reference period.* CI *is the 95% confidence interval of the change (equations S1 and S2), both change and* CI *in units given to the left. Number of sites is* $N_{\mathrm{sp}}$ *entering equation S2.*

| | | ***affected*** | ***affected* crop** | ***affected* forest** | ***affected* grass** | ***affected* peat** | ***other*** |
|---|---|---|---|---|---|---|---|
| $P$ (mm) | change | **-180** | **-125** | **-207** | **-169** | **-140** | **+100** |
| | CI | ±28 | ±74 | ±39 | ±68 | ±58 | ±83 |
| | relative | **-22.9%** | **-15.8%** | **-27.3%** | **-16.9%** | **-21.4%** | **13.6%** |
| | sites | 46 | 7 | 26 | 7 | 6 | 10 |
| $ET_0$ (mm) | change | **+105** | **+91** | **+109** | **+103** | **+107** | **-48** |
| | CI | ±8 | ±26 | ±12 | ±15 | ±20 | ±42 |
| | relative | **16.0%** | **12.6%** | **17.1%** | **14.4%** | **17.8%** | **-4.5%** |
| | sites | 46 | 7 | 26 | 7 | 6 | 10 |
| $T_{\mathrm{air}}$ (°C) | change | **+0.82** | **+0.92** | **+0.80** | **+0.93** | **+0.66** | +0.05 |
| | CI | ±0.13 | ±0.43 | ±0.17 | ±0.17 | ±0.55 | ±0.32 |
| | sites | 46 | 7 | 26 | 7 | 6 | 10 |
| $R_{\mathrm{g}}$ (MJ m$^{-2}$ yr$^{-1}$) | change | **+360** | **+307** | **+357** | **+353** | **+442** | **-147** |
| | CI | ±32 | ±84 | ±45 | ±51 | ±96 | ±95 |
| | relative | **9.2%** | **7.4%** | **9.5%** | **8.3%** | **11.9%** | **-2.7%** |
| | sites | 46 | 7 | 26 | 7 | 6 | 10 |
| $SW_{\mathrm{out}}$ (MJ m$^{-2}$ yr$^{-1}$) | change | **+69** | +32 | **+49** | **+103** | **+148** | -29 |
| | CI | ±21 | ±62 | ±15 | ±63 | ±123 | ±67 |
| | relative | **11.5%** | 4.0% | **11.8%** | **10.5%** | **25.3%** | -2.6% |
| | sites | 35 | 5 | 20 | 5 | 5 | 7 |
| albedo | change | +0.004 | -0.007 | +0.002 | +0.003 | +0.020 | +0.001 |
| | CI | ±0.005 | ±0.014 | ±0.004 | ±0.015 | ±0.026 | ±0.014 |
| | relative | 2.3% | -3.4% | 2.0% | 1.2% | 12.1% | 0.2% |
| | sites | 35 | 5 | 20 | 5 | 5 | 7 |
| $LW_{\mathrm{in}}$ (MJ m$^{-2}$ yr$^{-1}$) | change | +24 | **+87** | +32 | -29 | -17 | **+155** |
| | CI | ±30 | ±77 | ±37 | ±52 | ±148 | ±73 |
| | relative | 0.2% | 0.9% | 0.3% | -0.3% | -0.2% | 1.6% |
| | sites | 44 | 6 | 26 | 7 | 5 | 10 |
| $LW_{\mathrm{out}}$ (MJ m$^{-2}$ yr$^{-1}$) | change | **+148** | **+227** | **+153** | **+169** | +33 | -6 |
| | CI | ±29 | ±85 | ±25 | ±48 | ±204 | ±106 |
| | relative | **1.3%** | **2.0%** | **1.4%** | **1.5%** | 0.3% | 0.0% |
| | sites | 35 | 5 | 20 | 5 | 5 | 6 |
| $R_{\mathrm{n}}$ (MJ m$^{-2}$ yr$^{-1}$) | change | **+123** | **+141** | +98 | **+140** | **+177** | +16 |
| | CI | ±60 | ±87 | ±100 | ±80 | ±126 | ±53 |
| | relative | **6.3%** | **7.8%** | 4.7% | **7.9%** | **9.6%** | 0.6% |
| | sites | 36 | 5 | 20 | 5 | 6 | 7 |

*Table S2 continued*

| | | ***affected*** | ***affected* crop** | ***affected* forest** | ***affected* grass** | ***affected* peat** | ***other*** |
|---|---|---|---|---|---|---|---|
| EBC (filled) | change | **+0.02** | -0.02 | **+0.04** | +0.00 | +0.04 | +0.04 |
| | CI | ±0.02 | ±0.05 | ±0.03 | ±0.03 | ±0.07 | ±0.13 |
| | relative | **3.0%** | -2.7% | **4.9%** | -0.6% | 5.2% | 4.9% |
| | sites | 45 | 7 | 25 | 7 | 6 | 9 |
| $H$ (MJ m$^{-2}$ yr$^{-1}$) | change | **+169** | **+135** | **+235** | **+79** | +30 | -34 |
| | CI | ±36 | ±97 | ±52 | ±33 | ±58 | ±120 |
| | relative | **32.3%** | **43.5%** | **34.2%** | **28.9%** | 8.2% | -3.2% |
| | sites | 46 | 7 | 26 | 7 | 6 | 10 |
| $\lambda ET$ (MJ m$^{-2}$ yr$^{-1}$) | change | 0 | **-122** | -29 | +54 | **+205** | -9 |
| | CI | ±39 | ±118 | ±49 | ±68 | ±94 | ±123 |
| | relative | 0.0% | **-10.2%** | -2.8% | 4.4% | **20.8%** | -0.7% |
| | sites | 46 | 7 | 26 | 7 | 6 | 10 |
| $\lambda ET\ (H+\lambda ET)^{-1}$ | change | **-0.07** | **-0.10** | **-0.09** | **-0.05** | +0.03 | +0.03 |
| | CI | ±0.02 | ±0.08 | ±0.03 | ±0.04 | ±0.05 | ±0.04 |
| | relative | **-10.5%** | **-12.4%** | **-14.5%** | **-5.8%** | 3.3% | 5.3% |
| | sites | 44 | 7 | 26 | 6 | 5 | 10 |
| $S_l$ (MJ m$^{-2}$ yr$^{-1}$) | change | **+9.3** | **+33.4** | **+4.8** | **+17.0** | -7.8 | -6.8 |
| | CI | ±4.6 | ±26.1 | ±2.6 | ±9.6 | ±13.5 | ±17.3 |
| | relative | **299.2%** | **1384.2%** | **256.8%** | **110.4%** | -156.9% | -63.8% |
| | sites | 46 | 7 | 26 | 7 | 6 | 10 |
| $E_c$ (MJ m$^{-2}$ yr$^{-1}$) | change | **-1.6** | -2.1 | -1.0 | **-2.9** | -2.1 | +0.4 |
| | CI | ±1.1 | ±5.2 | ±1.4 | ±1.9 | ±2.9 | ±3.1 |
| | relative | **-17.8%** | -32.4% | -8.3% | **-44.0%** | -74.9% | 7.5% |
| | sites | 46 | 7 | 26 | 7 | 6 | 10 |
| IWUE* (gC hPa kg$^{-1}$ $H_2O$) | change | **+3.1** | **+2.8** | **+3.8** | **+2.5** | **+1.0** | +0.1 |
| | CI | ±0.5 | ±1.0 | ±0.7 | ±0.9 | ±0.7 | ±1.5 |
| | relative | **31.4%** | **32.6%** | **35.3%** | **20.7%** | **21.2%** | 0.4% |
| | sites | 45 | 6 | 26 | 7 | 6 | 10 |
| $WUE_{eco}$ | change | **-0.0011** | -0.0015 | -0.0002 | **-0.0027** | -0.0023 | +0.0004 |
| | CI | ±0.0009 | ±0.0043 | ±0.0012 | ±0.0013 | ±0.0026 | ±0.0021 |
| | relative | **-13.8%** | -27.7% | -2.3% | **-48.7%** | -88.5% | 9.0% |
| | sites | 46 | 7 | 26 | 7 | 6 | 10 |
| *swc* (cm$^3$ cm$^{-3}$) | change | **-0.051** | **-0.057** | **-0.044** | **-0.073** | **-0.038** | **+0.032** |
| | CI | ±0.010 | ±0.049 | ±0.014 | ±0.011 | ±0.034 | ±0.028 |
| | relative | **-16.2%** | **-19.8%** | **-17.0%** | **-18.6%** | **-5.5%** | **15.5%** |
| | sites | 33 | 5 | 20 | 6 | 2 | 9 |

## (b) Energy balance closure

Eddy-Covariance measurements are known for a gap in the energy balance closure (EBC): the sum of $H$ and $\lambda ET$ is frequently about 15 to 30% smaller than $R_n$ - $S_l$ - $E_c$ [58, 64]. Current theory suggests a number of different reasons including underestimation of the turbulent heat fluxes due to surface heterogeneity or incomplete correction of spectral losses, or unaccounted energy storage [64-68]. However, there is no consensus yet on the application of a correction, its distribution between $H$ and $\lambda ET$ and its implications for $E_c$ [69, 70]. However, relative changes in turbulent fluxes between years remain unaffected as long as EBC does not change systematically between respective years. Figure S1 demonstrates there was little average change in EBC, with a closure gap around 20% both in the reference period and in 2018. EBC slightly improved during the drought, although both increase and decrease were found for individual sites.

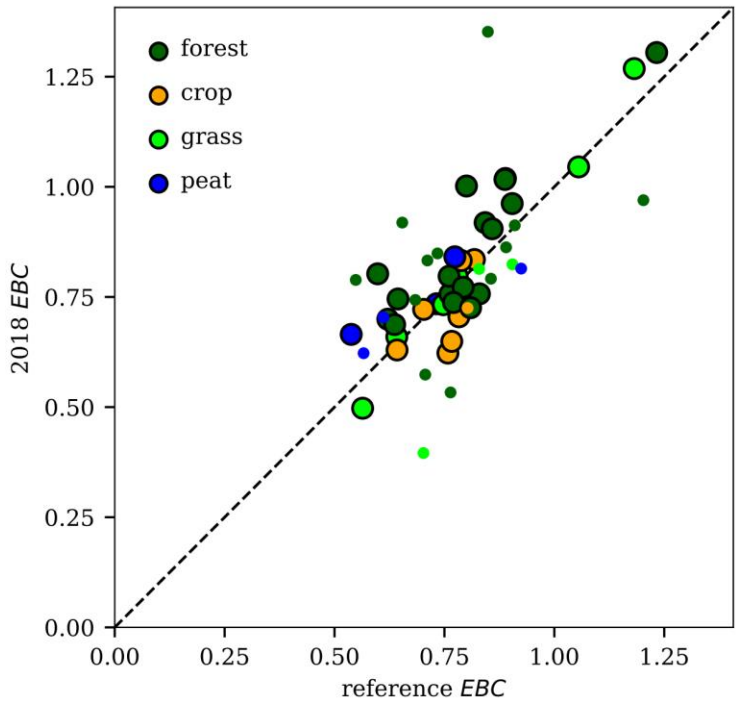


Figure S1: Energy balance closure (EBC), i.e., annual cumulative $(H+\lambda ET)(R_n-S_l-E_c)^{-1}$, compared between 2018 and the reference period for each site. Large symbols indicate sites where measurements of these variables were jointly available during both periods, small symbols indicate sites where $R_n$-$S_l$ was estimated from gap-filled short-wave incoming radiation according to [59]. Mean EBC across sites changed from 0.77 (reference) to 0.81 (2018) for the high-quality and from 0.77 to 0.80 for the filled records.

## (c) Intra-annual temporal dynamics of *ET*

On average, grassland sites showed higher evapotranspiration losses compared to the reference period in the early stages of the drought, and lower ones later presumably caused by soil water depletion. As a result, sensible heat fluxes were particularly high compared to the reference period during late stages of the drought (figure S2). Forests showed less extreme relative changes, in accordance with [71]. However, it should also be noted that on average forests showed higher sensible heat fluxes than grasslands both during the reference period and 2018, partly because of having a lower albedo. Any mitigation strategy by land use change would need to carefully consider this drawback effect. Cropland sites showed an even stronger tendency of evapotranspiration to decline during later stages of the drought. Inspection of a single cropland site demonstrates that this effect is at least partly due to earlier maturity and harvest, and strongly reduced evaporation from the dry topsoil after harvest (figure S2).

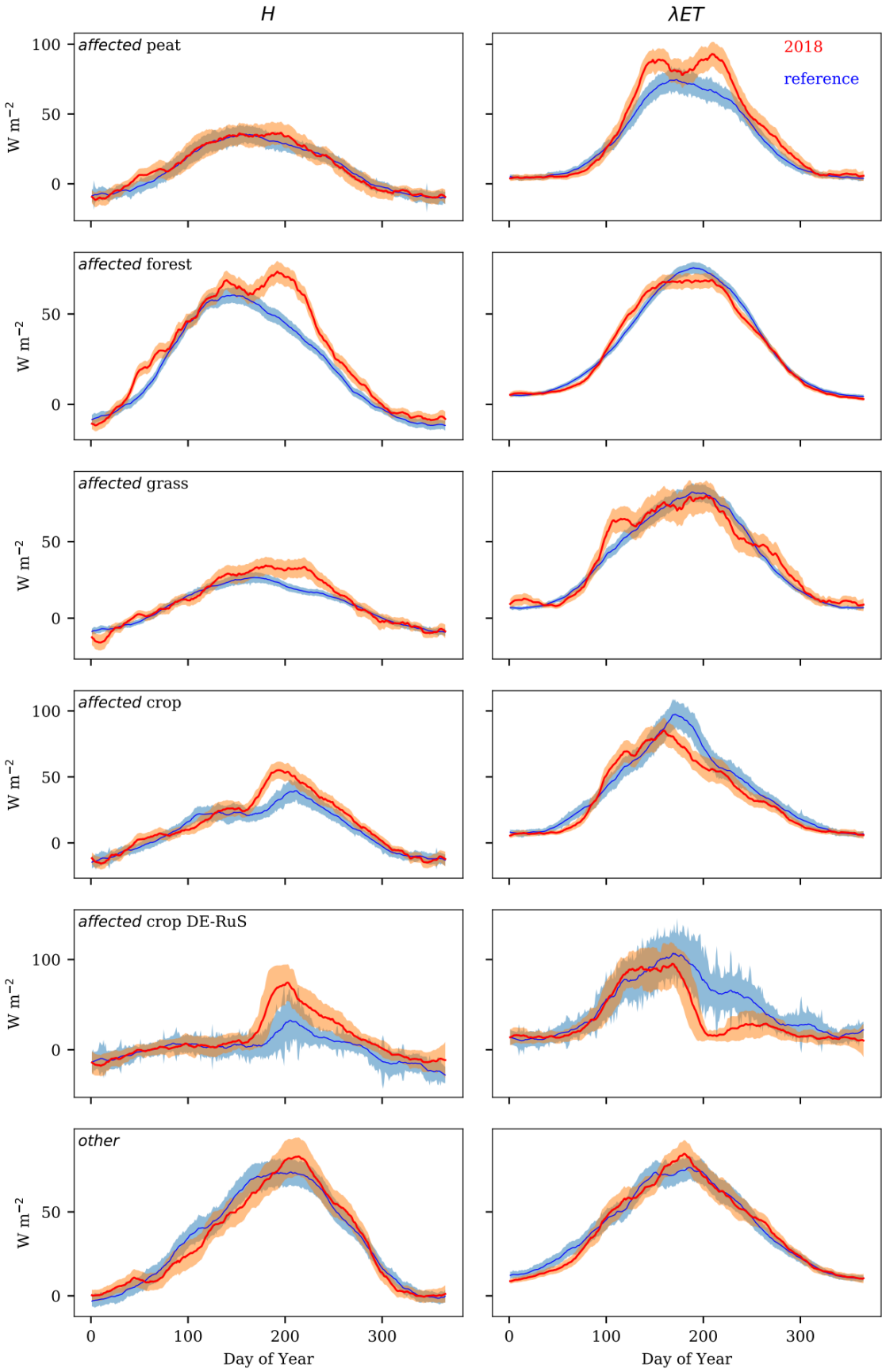


Figure S2: Annual course of sensible (*H*, *left column*) and latent heat flux (*λET*, right column, W $m^{-2}$) averaged across groups of ecosystems as a 30-day rolling average during 2018 (red) and the reference period (blue). Shaded areas indicate the 95% confidence interval estimated from variability within the 30-day rolling window, between reference years and between sites (see supplementary material a). Harvest of winter wheat at DE-RuS took place at Day of Year 197 in 2018, while in the two reference years it took place at Day 223 and 215, respectively.

## References

[1] Gielen B, De Vos B, Campioli M, Neirynck J, Papale D, Verstraeten A, Ceulemans R,Janssens IA. 2013 Biometric and eddy covariance-based assessment of decadal carbon sequestration of a temperate Scots pine forest. *Agric. For. Meteorol.* **174**, 135-143. (DOI:10.1016/j.agrformet.2013.02.008).

[2] Buysse P, Bodson B, Debacq A, De Ligne A, Heinesch B, Manise T, Moureaux C,Aubinet M. 2017 Carbon budget measurement over 12 years at a crop production site in the silty-loam region in Belgium. *Agric. For. Meteorol.* **246**, 241-255. (DOI:10.1016/j.agrformet.2017.07.004).

[3] Aubinet M, Hurdebise Q, Chopin H, Debacq A, De Ligne A, Heinesch B, Manise T,Vincke C. 2018 Inter-annual variability of Net Ecosystem Productivity for a temperate mixed forest: A predominance of carry-over effects? *Agric. For. Meteorol.* **262**, 340-353. (DOI:10.1016/j.agrformet.2018.07.024).

[4] Zeeman MJ, Hiller R, Gilgen AK, Michna P, Pluss P, Buchmann N,Eugster W. 2010 Management and climate impacts on net CO2 fluxes and carbon budgets of three grasslands along an elevational gradient in Switzerland. *Agric. For. Meteorol.* **150**, 519-530. (DOI:10.1016/j.agrformet.2010.01.011).

[5] Hortnagl L, Barthel M, Buchmann N, Eugster W, Butterbach-Bahl K, Diaz-Pines E, Zeeman M, Klumpp K, Kiese R, Bahn M, et al. 2018 Greenhouse gas fluxes over managed grasslands in Central Europe. *Global Change Biology* **24**, 1843-1872. (DOI:10.1111/gcb.14079).

[6] Haeni M, Zweifel R, Eugster W, Gessler A, Zielis S, Bernhofer C, Carrara A, Grunwald T, Havrankova K, Heinesch B, et al. 2017 Winter respiratory C losses provide explanatory power for net ecosystem productivity. *J. Geophys. Res.-Biogeosci.* **122**, 243-260. (DOI:10.1002/2016jg003455).

[7] Emmel C, Winkler A, Hortnagl L, Revill A, Ammann C, D'Odorico P, Buchmann N,Eugster W. 2018 Integrated management of a Swiss cropland is not sufficient to preserve its soil carbon pool in the long term. *Biogeosciences* **15**, 5377-5393. (DOI:10.5194/bg-15-5377-2018).

[8] Krupkova L, Markova I, Havrankova K, Pokorny R, Urban O, Sigut L, Pavelka M, Cienciala E,Marek MV. 2017 Comparison of different approaches of radiation use efficiency of biomass formation estimation in Mountain Norway spruce. *Trees-Struct. Funct.* **31**, 325-337. (DOI:10.1007/s00468-016-1486-2).

[9] Acosta M, Darenova E, Dusek J,Pavelka M. 2017 Soil carbon dioxide fluxes in a mixed floodplain forest in the Czech Republic. *Eur. J. Soil Biol.* **82**, 35-42. (DOI:10.1016/j.ejsobi.2017.08.006).

[10] McGloin R, Sigut L, Havrankova K, Dusek J, Pavelka M,Sedlak P. 2018 Energy balance closure at a variety of ecosystems in Central Europe with contrasting topographies. *Agric. For. Meteorol.* **248**, 418-431. (DOI:10.1016/j.agrformet.2017.10.003).

[11] Krupkova L, Havrankova K, Krejza J, Sedlak P,Marek MV. 2019 Impact of water scarcity on spruce and beech forests. *J. For. Res.* **30**, 899-909. (DOI:10.1007/s11676-018-0642-5).

[12] Dusek J, Cizkova H, Stellner S, Czerny R,Kvet J. 2012 Fluctuating water table affects gross ecosystem production and gross radiation use efficiency in a sedge-grass marsh. *Hydrobiologia* **692**, 57-66. (DOI:10.1007/s10750-012-0998-z).

[13] Heusinger J,Weber S. 2017 Surface energy balance of an extensive green roof as quantified by full year eddy-covariance measurements. *Sci. Total Environ.* **577**, 220-230. (DOI:10.1016/j.scitotenv.2016.10.168).

[14] Poyda A, Wizemann HD, Ingwersen J, Eshonkulov R, Hogy P, Demyan MS, Kremer P, Wulfmeyer V,Streck T. 2019 Carbon fluxes and budgets of intensive crop rotations in two regional climates of southwest Germany. *Agriculture Ecosystems & Environment* **276**, 31-46. (DOI:10.1016/j.agee.2019.02.011).

[15] Wizemann HD, Ingwersen J, Hogy P, Warrach-Sagi K, Streck T,Wulfmeyer V. 2015 Three year observations of water vapor and energy fluxes over agricultural crops in two regional climates of Southwest Germany. *Meteorologische Zeitschrift* **24**, 39-59. (DOI:10.1127/metz/2014/0618).

[16] Kiese R, Fersch B, Baessler C, Brosy C, Butterbach-Bahl K, Chwala C, Dannenmann M, Fu J, Gasche R, Grote R, et al. 2018 The TERENO Pre-Alpine Observatory: Integrating Meteorological, Hydrological, and Biogeochemical Measurements and Modeling. *Vadose Zone Journal* **17**, 17. (DOI:10.2136/vzj2018.03.0060).

[17] Anthoni PM, Freibauer A, Kolle O,Schulze ED. 2004 Winter wheat carbon exchange in Thuringia, Germany. *Agric. For. Meteorol.* **121**, 55-67. (DOI:10.1016/s0168-1923(03)00162-x).

[18] Prescher AK, Grunwald T,Bernhofer C. 2010 Land use regulates carbon budgets in eastern Germany: From NEE to NBP. *Agric. For. Meteorol.* **150**, 1016-1025. (DOI:10.1016/j.agrformet.2010.03.008).

[19] Knohl A, Schulze ED, Kolle O,Buchmann N. 2003 Large carbon uptake by an unmanaged 250-year-old deciduous forest in Central Germany. *Agric. For. Meteorol.* **118**, 151-167. (DOI:10.1016/s0168-1923(03)00115-1).

[20] Wollschlager U, Attinger S, Borchardt D, Brauns M, Cuntz M, Dietrich P, Fleckenstein JH, Friese K, Friesen J, Harpke A, et al. 2017 The Bode hydrological observatory: a platform for integrated, interdisciplinary hydro-ecological research within the TERENO Harz/Central German Lowland Observatory. *Environ. Earth Sci.* **76**, 25. (DOI:10.1007/s12665-016-6327-5).

[21] Koebsch F, Glatzel S, Hofmann J, Forbrich I,Jurasinski G. 2013 CO2 exchange of a temperate fen during the conversion from moderately rewetting to flooding. *J. Geophys. Res.-Biogeosci.* **118**, 940-950. (DOI:10.1002/jgrg.20069).

[22] Post H, Franssen HJH, Graf A, Schmidt M,Vereecken H. 2015 Uncertainty analysis of eddy covariance CO2 flux measurements for different EC tower distances using an extended two-tower approach. *Biogeosciences* **12**, 1205-1221. (DOI:10.5194/bg-12-1205-2015).

[23] Klosterhalfen A, Moene AF, Schmidt M, Scanlon TM, Vereecken H,Graf A. 2019 Sensitivity analysis of a source partitioning method for H2O and CO2 fluxes based on high frequency eddy covariance data: Findings from field data and large eddy simulations. *Agric. For. Meteorol.* **265**, 152 - 170. (DOI:10.1016/j.agrformet.2018.11.003).

[24] Ney P, Graf A, Bogena H, Diekkruger B, Drue C, Esser O, Heinemann G, Klosterhalfen A, Pick K, Putz T, et al. 2019 CO2 fluxes before and after partial deforestation of a Central European spruce forest. *Agric. For. Meteorol.* **274**, 61-74. (DOI:10.1016/j.agrformet.2019.04.009).

[25] Hommeltenberg J, Schmid HP, Drosler M,Werle P. 2014 Can a bog drained for forestry be a stronger carbon sink than a natural bog forest? *Biogeosciences* **11**, 3477-3493. (DOI:10.5194/bg-11-3477-2014).
[26] Franz D, Koebsch F, Larmanou E, Augustin J,Sachs T. 2016 High net CO2 and CH4 release at a eutrophic shallow lake on a formerly drained fen. *Biogeosciences* **13**, 3051-3070. (DOI:10.5194/bg-13-3051-2016).
[27] Wu J, Larsen KS, van der Linden L, Beier C, Pilegaard K,Ibrom A. 2013 Synthesis on the carbon budget and cycling in a Danish, temperate deciduous forest. *Agric. For. Meteorol.* **181**, 94-107. (DOI:10.1016/j.agrformet.2013.07.012).
[28] Luo YP, El-Madany TS, Filippa G, Ma XL, Ahrens B, Carrara A, Gonzalez-Cascon R, Cremonese E, Galvagno M, Hammer TW, et al. 2018 Using Near-Infrared-Enabled Digital Repeat Photography to Track Structural and Physiological Phenology in Mediterranean Tree-Grass Ecosystems. *Remote Sens.* **10**, 32. (DOI:10.3390/rs10081293).
[29] El-Madany TS, Reichstein M, Perez-Priego O, Carrara A, Moreno G, Martin MP, Pacheco-Labrador J, Wohlfahrt G, Nieto H, Weber U, et al. 2018 Drivers of spatio-temporal variability of carbon dioxide and energy fluxes in a Mediterranean savanna ecosystem. *Agric. For. Meteorol.* **262**, 258-278. (DOI:10.1016/j.agrformet.2018.07.010).
[30] Mammarella I, Launiainen S, Gronholm T, Keronen P, Pumpanen J, Rannik U,Vesala T. 2009 Relative Humidity Effect on the High-Frequency Attenuation of Water Vapor Flux Measured by a Closed-Path Eddy Covariance System. *Journal of Atmospheric and Oceanic Technology* **26**, 1856-1866. (DOI:10.1175/2009jtecha1179.1).
[31] Launiainen S, Katul GG, Kolari P, Lindroth A, Lohila A, Aurela M, Varlagin A, Grelle A,Vesala T. 2016 Do the energy fluxes and surface conductance of boreal coniferous forests in Europe scale with leaf area? *Global Change Biology* **22**, 4096-4113. (DOI:10.1111/gcb.13497).
[32] Rinne J, Tuittila ES, Peltola O, Li XF, Raivonen M, Alekseychik P, Haapanala S, Pihlatie M, Aurela M, Mammarella I, et al. 2018 Temporal Variation of Ecosystem Scale Methane Emission From a Boreal Fen in Relation to Temperature, Water Table Position, and Carbon Dioxide Fluxes. *Global Biogeochemical Cycles* **32**, 1087-1106. (DOI:10.1029/2017gb005747).
[33] Kulmala L, Pumpanen J, Kolari P, Dengel S, Berninger F, Koster K, Matkala L, Vanhatalo A, Vesala T,Back J. 2019 Inter- and intra-annual dynamics of photosynthesis differ between forest floor vegetation and tree canopy in a subarctic Scots pine stand. *Agric. For. Meteorol.* **271**, 1-11. (DOI:10.1016/j.agrformet.2019.02.029).
[34] Moreaux V, Lamaud E, Bosc A, Bonnefond JM, Medlyn BE,Loustau D. 2011 Paired comparison of water, energy and carbon exchanges over two young maritime pine stands (Pinus pinaster Ait.): effects of thinning and weeding in the early stage of tree growth. *Tree Physiology* **31**, 903-921. (DOI:10.1093/treephys/tpr048).
[35] Domeignoz-Horta LA, Spor A, Bru D, Breuil MC, Bizouard F, Leonard J,Philippot L. 2015 The diversity of the N2O reducers matters for the N2O:N-2 denitrification end-product ratio across an annual and a perennial cropping system. *Front. Microbiol.* **6**, 10. (DOI:10.3389/fmicb.2015.00971).
[36] Granier A, Breda N, Longdoz B, Gross P,Ngao J. 2008 Ten years of fluxes and stand growth in a young beech forest at Hesse, North-eastern France. *Annals of Forest Science* **65**, 13. (DOI:10.1051/forest:2008052).
[37] Vitale L, Di Tommasi P, Arena C, Riondino M, Forte A, Verlotta A, Fierro A, De Santo AV, Fuggi A,Magliulo V. 2009 Growth and gas exchange response to water shortage of a maize crop on different soil types. *Acta Physiol. Plant.* **31**, 331-341. (DOI:10.1007/s11738-008-0239-2).
[38] Fares S, Savi F, Muller J, Matteucci G,Paoletti E. 2014 Simultaneous measurements of above and below canopy ozone fluxes help partitioning ozone deposition between its various sinks in a Mediterranean Oak Forest. *Agric. For. Meteorol.* **198**, 181-191. (DOI:10.1016/j.agrformet.2014.08.014).
[39] Tezza L, Vendrame N,Pitacco A. 2019 Disentangling the carbon budget of a vineyard: The role of soil management. *Agriculture Ecosystems & Environment* **272**, 52-62. (DOI:10.1016/j.agee.2018.11.002).
[40] Hoshika Y, Fares S, Savi F, Gruening C, Goded I, De Marco A, Sicard P,Paoletti E. 2017 Stomatal conductance models for ozone risk assessment at canopy level in two Mediterranean evergreen forests. *Agric. For. Meteorol.* **234**, 212-221. (DOI:10.1016/j.agrformet.2017.01.005).
[41] Galvagno M, Wohlfahrt G, Cremonese E, Rossini M, Colombo R, Filippa G, Julitta T, Manca G, Siniscalco C, di Cella UM, et al. 2013 Phenology and carbon dioxide source/sink strength of a subalpine grassland in response to an exceptionally short snow season. *Environ. Res. Lett.* **8**, 10. (DOI:10.1088/1748-9326/8/2/025008).
[42] Elbers JA, Jacobs CMJ, Kruijt B, Jans WWP,Moors EJ. 2011 Assessing the uncertainty of estimated annual totals of net ecosystem productivity: A practical approach applied to a mid latitude temperate pine forest. *Agric. For. Meteorol.* **151**, 1823-1830. (DOI:10.1016/j.agrformet.2011.07.020).
[43] Mamkin V, Kurbatova J, Avilov V, Ivanov D, Kuricheva O, Varlagin A, Yaseneva I,Olchev A. 2019 Energy and CO2 exchange in an undisturbed spruce forest and clear-cut in the Southern Taiga. *Agric. For. Meteorol.* **265**, 252-268. (DOI:10.1016/j.agrformet.2018.11.018).
[44] Kurbatova J, Tatarinov F, Molchanov A, Varlagin A, Avilov V, Kozlov D, Ivanov D,Valentini R. 2013 Partitioning of ecosystem respiration in a paludified shallow-peat spruce forest in the southern taiga of European Russia. *Environ. Res. Lett.* **8**, 9. (DOI:10.1088/1748-9326/8/4/045028).
[45] Nilsson M, Sagerfors J, Buffam I, Laudon H, Eriksson T, Grelle A, Klemedtsson L, Weslien P,Lindroth A. 2008 Contemporary carbon accumulation in a boreal oligotrophic minerogenic mire - a significant sink after accounting for all C-fluxes. *Global Change Biology* **14**, 2317-2332. (DOI:10.1111/j.1365-2486.2008.01654.x).
[46] van Meeningen Y, Wang M, Karlsson T, Seifert A, Schurgers G, Rinnan R,Hoist T. 2017 Isoprenoid emission variation of Norway spruce across a European latitudinal transect. *Atmospheric Environment* **170**, 45-57. (DOI:10.1016/j.atmosenv.2017.09.045).
[47] Lindroth A, Holst J, Heliasz M, Vestin P, Lagergren F, Biermann T, Cai ZZ,Molder M. 2018 Effects of low thinning on carbon dioxide fluxes in a mixed hemiboreal forest. *Agric. For. Meteorol.* **262**, 59-70. (DOI:10.1016/j.agrformet.2018.06.021).
[48] Jocher G, Marshall J, Nilsson MB, Linder S, De Simon G, Hornlund T, Lundmark T, Nasholm T, Lofvenius MO, Tarvainen L, et al. 2018 Impact of Canopy Decoupling and Subcanopy Advection on the Annual Carbon Balance of a Boreal Scots Pine Forest as Derived From Eddy Covariance. *J. Geophys. Res.-Biogeosci.* **123**, 303-325. (DOI:10.1002/2017jg003988).

[49] Chi JS, Nilsson MB, Kljun N, Wallerman J, Fransson JES, Laudon H, Lundmark T,Peichl M. 2019 The carbon balance of a managed boreal landscape measured from a tall tower in northern Sweden. *Agric. For. Meteorol.* **274**, 29-41. (DOI:10.1016/j.agrformet.2019.04.010).

[50] Reichstein M, Falge E, Baldocchi D, Papale D, Aubinet M, Berbigier P, Bernhofer C, Buchmann N, Gilmanov T, Granier A, et al. 2005 On the separation of net ecosystem exchange into assimilation and ecosystem respiration: review and improved algorithm. *Global Change Biology* **11**, 1424-1439. (DOI:10.1111/j.1365-2486.2005.001002.x).

[51] Papale D, Reichstein M, Aubinet M, Canfora E, Bernhofer C, Kutsch W, Longdoz B, Rambal S, Valentini R, Vesala T, et al. 2006 Towards a standardized processing of Net Ecosystem Exchange measured with eddy covariance technique: algorithms and uncertainty estimation. *Biogeosciences* **3**, 571-583. (DOI:10.5194/bg-3-571-2006).

[52] Lasslop G, Reichstein M, Papale D, Richardson AD, Arneth A, Barr A, Stoy P,Wohlfahrt G. 2010 Separation of net ecosystem exchange into assimilation and respiration using a light response curve approach: critical issues and global evaluation. *Global Change Biology* **16**, 187-208. (DOI:10.1111/j.1365-2486.2009.02041.x).

[53] Graf A, Bogena HR, Drue C, Hardelauf H, Putz T, Heinemann G,Vereecken H. 2014 Spatiotemporal relations between water budget components and soil water content in a forested tributary catchment. *Water Resources Research* **50**, 4837-4857. (DOI:10.1002/2013wr014516).

[54] Graf A. 2017 Gap-filling meteorological variables with Empirical Orthogonal Functions. In *EGU 2017 General Assembly* (23 Apr 2017 - 28 Apr 2017, Vienna (Austria).

[55] Wutzler T, Lucas-Moffat A, Migliavacca M, Knauer J, Sickel K, Sigut L, Menzer O,Reichstein M. 2018 Basic and extensible post-processing of eddy covariance flux data with REddyProc. *Biogeosciences* **15**, 5015-5030. (DOI:10.5194/bg-15-5015-2018).

[56] Drought 2018 Team and ICOS Ecosystem Thematic Centre. 2020 Drought-2018 ecosystem eddy covariance flux product for 52 stations in FLUXNET-Archive format (DOI:10.18160/YVR0-4898)

[57] Webster R. 1997 Regression and functional relations. *European Journal of Soil Science* **48**, 557-566.

[58] Wilson K, Goldstein A, Falge E, Aubinet M, Baldocchi D, Berbigier P, Bernhofer C, Ceulemans R, Dolman H, Field C, et al. 2002 Energy balance closure at FLUXNET sites. *Agric. For. Meteorol.* **113**, 223-243. (DOI:10.1016/s0168-1923(02)00109-0).

[59] Allen RG, Pereira LS, Raes D,Smith M. 1998 *Crop evapotranspiration: Guidelines for computing crop water requirements*. Rome, FAO; 300 p.

[60] Ciais P, Reichstein M, Viovy N, Granier A, Ogee J, Allard V, Aubinet M, Buchmann N, Bernhofer C, Carrara A, et al. 2005 Europe-wide reduction in primary productivity caused by the heat and drought in 2003. *Nature* **437**, 529-533.

[61] Finkelstein PL,Sims PF. 2001 Sampling error in eddy correlation flux measurements. *Journal of Geophysical Research-Atmospheres* **106**, 3503-3509. (DOI:10.1029/2000jd900731).

[62] Pastorello G,Trotta C,Canfora E,Chu H,Christianson D,Cheah Y-W,Poindexter C,Chen J,Elbashandy A,Humphrey M, et al. 2020 The FLUXNET2015 dataset and the ONEFlux processing pipeline for eddy covariance data. *Scientific Data* **7**, 225. (DOI:10.1038/s41597-020-0534-3).

[63] Kish L. 1965 *Survey sampling*. New York, Wiley; 643 p.

[64] Stoy PC, Mauder M, Foken T, Marcolla B, Boegh E, Ibrom A, Arain MA, Arneth A, Aurela M, Bernhofer C, et al. 2013 A data-driven analysis of energy balance closure across FLUXNET research sites: The role of landscape scale heterogeneity. *Agric. For. Meteorol.* **171-172**, 137-152. (DOI:10.1016/j.agrformet.2012.11.004).

[65] Eder F, Schmidt M, Damian T, Traumner K,Mauder M. 2015 Mesoscale Eddies Affect Near-Surface Turbulent Exchange: Evidence from Lidar and Tower Measurements. *Journal of Applied Meteorology and Climatology* **54**, 189-206. (DOI:10.1175/jamc-d-14-0140.1).

[66] Eshonkulov R, Poyda A, Ingwersen J, Wizemann HD, Weber TKD, Kremer P, Hogy P, Pulatov A,Streck T. 2019 Evaluating multi-year, multi-site data on the energy balance closure of eddy-covariance flux measurements at cropland sites in southwestern Germany. *Biogeosciences* **16**, 521-540. (DOI:10.5194/bg-16-521-2019).

[67] Kidston J, Brümmer C, Black TA, Morgenstern K, Nesic Z, McCaughey JH,Barr AG. 2010 Energy Balance Closure Using Eddy Covariance Above Two Different Land Surfaces and Implications for CO2 Flux Measurements. *Bound.-Layer Meteor.* **136**, 193-218. (DOI:10.1007/s10546-010-9507-y).

[68] Haverd V, Cuntz M, Leuning R,Keith H. 2007 Air and biomass heat storage fluxes in a forest canopy: Calculation within a soil vegetation atmosphere transfer model. *Agric. For. Meteorol.* **147**, 125-139. (DOI:10.1016/j.agrformet.2007.07.006).

[69] Foken T. 2008 The energy balance closure problem: An overview. *Ecological Applications* **18**, 1351-1367. (DOI:10.1890/06-0922.1).

[70] Foken T, Aubinet M, Finnigan JJ, Leclerc MY, Mauder M,U KTP. 2011 Results of a Panel Discussion About the Energy Balance Closure Correction for Trace Gases. *Bulletin of the American Meteorological Society* **92**, ES13-ES18.

[71] Teuling AJ, Seneviratne SI, Stockli R, Reichstein M, Moors E, Ciais P, Luyssaert S, van den Hurk B, Ammann C, Bernhofer C, et al. 2010 Contrasting response of European forest and grassland energy exchange to heatwaves. *Nat. Geosci.* **3**, 722-727. (DOI:10.1038/ngeo950).